These findings raise the possibility that transplanted MSCs have beneficial effects on myocardial structure and function via myogenesis and angiogenesis. However, little information is available about the therapeutic potential of MSCs for DCM.

A unique model of myocarditis in the rat has been created by immunization with porcine cardiac myosin,[13] which results in severe heart failure characterized by increased cardiac fibrosis and left ventricular (LV) dilation.[14] Thus, the late phase of this model can serve as a model of DCM.

The purpose of this study was to investigate the following topics: (1) whether transplantation of MSCs induces myogenesis and angiogenesis, decreases collagen deposition in the myocardium, and thereby improves cardiac function in a rat model of DCM and (2) whether the beneficial effects of MSCs are mediated by their differentiation into cardiomyocytes and vascular cells and/or by their supplying angiogenic, antiapoptotic, and mitogenic factors.

Methods

Expansion of Bone Marrow MSCs

MSC expansion was performed according to previously described methods.[4] In brief, we humanely killed male Lewis rats and harvested bone marrow by flushing their femoral and tibial cavities with phosphate-buffered saline (PBS). Bone marrow cells were cultured in α-minimal essential medium supplemented with 10% fetal bovine serum and antibiotics. A small number of cells developed visible symmetric colonies by days 5 to 7. Nonadherent hematopoietic cells were removed, and the medium was replaced. The adherent, spindle-shaped MSC population expanded to $>5\times10^7$ cells within $\approx$4 to 5 passages after the cells were first plated.

Flow Cytometry

Cultured MSCs were analyzed by fluorescence-activated cell sorting (FACS) (FACScan flow cytometer, Becton Dickinson). Cells were incubated with fluorescein isothiocyanate (FITC)–conjugated mouse monoclonal antibodies against rat CD31 (clone TLD-3A12, Becton Dickinson), CD34 (clone ICO-115, Santa Cruz), CD45 (clone OX-1, Becton Dickinson), CD90 (clone OX-7, Becton Dickinson), vimentin (clone V9, Dako), and smooth muscle actin (SMA; clone 1A4, Dako). FITC-conjugated hamster anti-rat CD29 monoclonal antibody (clone Ha2/5, Becton Dickinson) and rabbit anti-rat c-Kit polyclonal antibody (clone C-19, Santa Cruz) were used. Isotype-identical antibodies served as controls.

Model of DCM

Male Lewis rats weighing 220 to 250 g (Japan SLC Inc, Hamamatsu, Japan) were used in this study. These isogenic rats served as donors and recipients of MSCs to simulate autologous implantation. DCM was produced by inducing experimental myocarditis, as described previously.[13,14] In brief, 1 mg (0.1 mL) of porcine heart myosin (Sigma) was mixed with an equal volume of Freund's complete adjuvant (Sigma) and injected into a footpad on days 1 and 7. Five weeks after immunization, these rats served as a model of heart failure due to DCM.

MSC Transplantation

In a preliminary experiment, we performed dose-response studies to obtain the maximal effects of cell transplantation. Because the effect of 10^6 MSCs was modest, we used 5×10^6 MSCs for transplantation. Five weeks after immunization, we injected a total of 5×10^6 MSCs/100 μL PBS, or PBS alone, into the myocardium at 10 points. In brief, the LV was divided into 3 levels (basal, middle, and apical). The basal and middle levels were each subdivided into 4 segments, and the apical level was subdivided into 2 segments. Injection into each segment was performed with a 27-gauge needle. Sham rats received intramyocardial injections of 100 μL PBS. This protocol resulted in the creation of 3 groups: DCM rats given MSCs (MSC-treated DCM group, n=10); DCM rats given PBS (untreated DCM group, n=10); and sham rats given PBS (sham group, n=10). The Animal Care Committee of the National Cardiovascular Center approved this experimental protocol.

Echocardiographic Studies

Echocardiographic studies were performed by an investigator, blinded to treatment allocation, at 5 weeks after immunization (before treatment) and 4 weeks after cell transplantation (after treatment). Two-dimensional, targeted M-mode tracings were obtained at the level of the papillary muscles with an echocardiographic system equipped with a 7.5-MHz transducer (HP Sonos 5500, Hewlett-Packard).[15] LV dimensions were measured according to the American Society for Echocardiology leading-edge method from at least 3 consecutive cardiac cycles. Fractional shortening was calculated as (LVDd−LVDs)/LVDd×100, where LVDd=LV diastolic dimension and LVDs=LV systolic dimension.

Hemodynamic Studies

Hemodynamic studies were performed 4 weeks after cell transplantation. A 1.5F micromanometer-tipped catheter (Millar Instruments) was inserted into the right carotid artery for measurement of mean arterial pressure.[16] Next, the catheter was advanced into the LV for measurement of LV pressure. Hemodynamic variables were measured with a pressure transducer (model P23 ID, Gould) connected to a polygraph. After completion of these measurements, the left and right ventricles were excised and weighed.

Histological Examination

To detect fibrosis in cardiac muscle, the LV myocardium (n=5 from each group) was fixed in 10% formalin, cut transversely, embedded in paraffin, and stained with Masson's trichrome. Transverse sections were randomly obtained from the 3 levels (basal, middle, and apical), and 20 randomly selected fields per section (n=60 per animal) were analyzed. After each field was scanned and computerized with a digital image analyzer (WinRoof, Mitani Co), collagen volume fraction was calculated as the sum of all areas containing connective tissue divided by the total area of the image.[15]

To detect capillaries in the myocardium, samples of harvested muscle (n=5 each) were embedded in OCT compound (Miles Scientific), snap-frozen in LN_2, cut into transverse sections, and stained for alkaline phosphatase by an indoxyltetrazolium method. Transverse sections were randomly obtained from the 3 levels (basal, middle, and apical), and 5 randomly selected fields per section (n=15 per animal) were analyzed. The number of capillaries was counted by light microscopy at a magnification of ×200. The number of capillaries in each field was averaged and expressed as the number of capillary vessels. These morphometric studies were performed by 2 examiners who were blinded to treatment assignment.

Assessment of Cell Differentiation

Suspended MSCs were labeled with fluorescent dyes with use of a PKH26 red fluorescent cell linker kit (Sigma), as reported previously.[17] Fluorescence-labeled MSCs were injected into the myocardium 5 weeks after immunization. Rats (n=5) were humanely killed 4 weeks after cell transplantation. LV samples were embedded in OCT compound, snap-frozen in LN_2, and cut into sections. Immunofluorescence staining was performed with monoclonal mouse anti-cardiac troponin T (Novo), anti-desmin (Dako), anti-connexin-43 (Sigma), polyclonal rabbit anti–von Willebrand factor (Dako), and monoclonal mouse SMA (Dako). FITC-conjugated IgG antibody (BD Pharmingen) was used as a secondary antibody. To perform quantitative analysis of the magnitude of MSC differentiation into cardiomyocytes, heart cells from each rat (n=5) were isolated by incubation in balanced salt solution containing 0.06% collagenase type II (Worthington Biochemical Co), as reported previously.[18] PKH26/troponin T double-positive cells were detected by FACS.

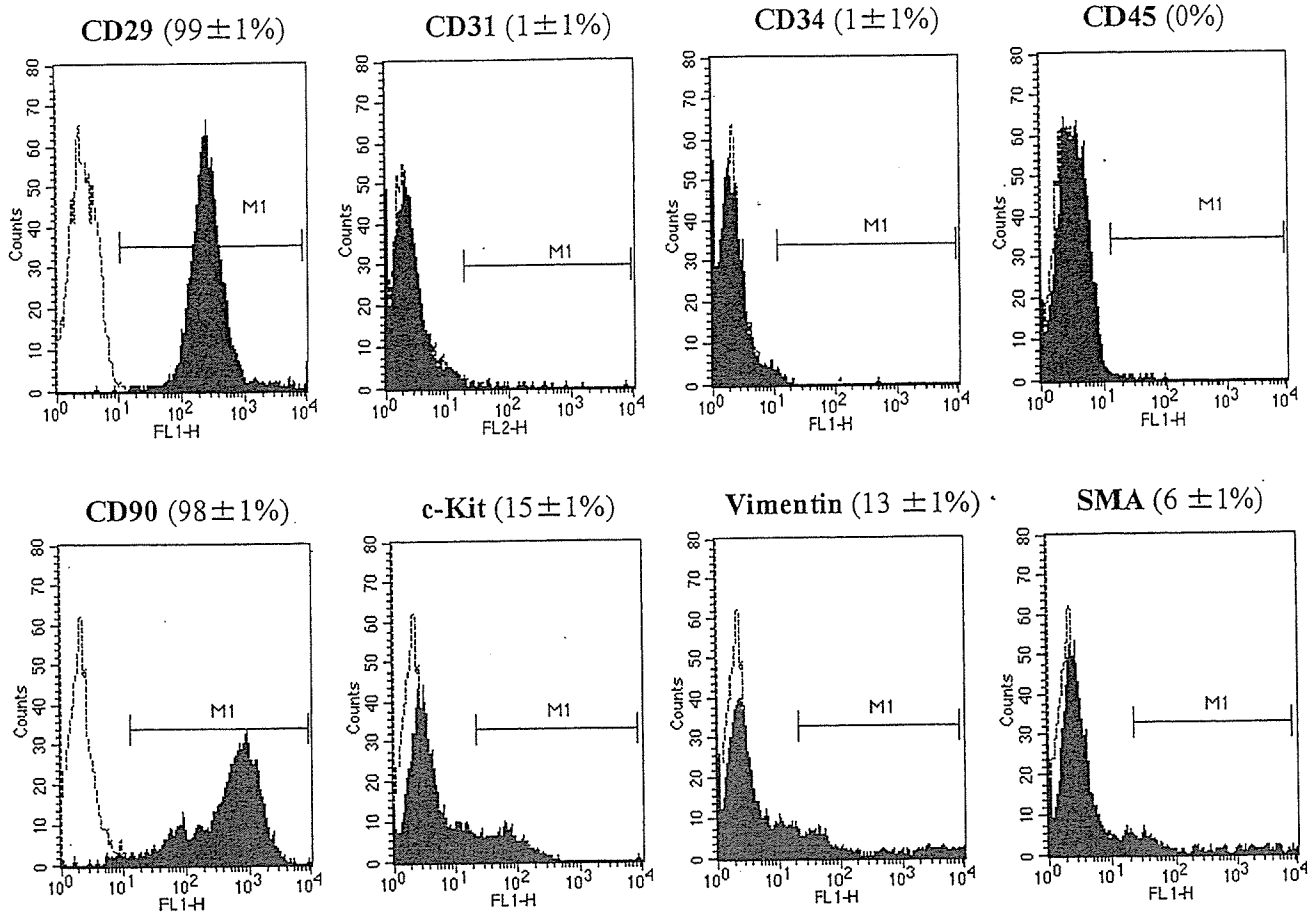

Figure 1. Flow-cytometric analysis of the adherent, spindle-shaped MSC population expanded to 4 to 5 passages. Most of the MSCs expressed CD29 and CD90, whereas they were negative for CD31, CD34, CD45, and SMA. Some of the cells were positive for c-Kit and vimentin.

Western Blot Analysis of Matrix Metalloproteinases

To identify the protein expression of matrix metalloproteinases (MMPs)-2 and -9, Western blotting was performed with rabbit polyclonal antibody raised against MMP-2 (Laboratory vision Co) and MMP-9 (Chemicon Co). The LV obtained from individual rats was used for comparison among the 3 groups (n=5 each). These samples were homogenized on ice in 0.1% Tween 20 homogenization buffer with a protease inhibitor. Then, 40 μg of protein was transferred into sample buffer, loaded on a 7.5% sodium dodecyl sulfate–polyacrylamide gel, and blotted onto a polyvinylidene fluoride membrane (Millipore Co). After being blocked for 120 minutes, the membrane was incubated with primary antibody at a dilution of 1:200. The membrane was incubated with peroxidase labeled with secondary antibody at a dilution of 1:1000. Positive protein bands were visualized with an ECL kit (Amersham) and measured by densitometry. Western blot analysis with a mouse polyclonal antibody raised against β-actin (Santa Cruz) was used as a protein loading control.

Assay for Angiogenic, Antiapoptotic, and Mitogenic Factors

To investigate whether MSCs produce angiogenic and growth factors, we measured VEGF, hepatocyte growth factor (HGF), insulin-like growth factor-1 (IGF-1), and adrenomedullin (AM) levels in conditioned medium 24 hours after medium replacement. VEGF, HGF, and IGF-1 were measured by enzyme immunoassay (VEGF immunoassay, R&D Systems Inc; rat HGF enzyme immunoassay, Institute of Immunology Co, Ltd; and active rat IGF-1 enzyme immunoassay, Diagnostic Systems Laboratories, Inc). AM level was measured with a radioimmunoassay kit (Shionogi Co), as reported previously.[19] The amounts of these products produced by MSCs were compared with those produced by bone marrow–derived mononuclear cells (MNCs) because MNCs have commonly been used for regenerative therapy.[19–21] There was no significant difference in cell viability between MSCs and MNCs 24 hours after seeding (88±5% versus 85±4% by trypan blue solution). In vivo, circulating levels of VEGF, HGF, IGF-1, and AM were measured before and 24 hours after administration of MSCs or vehicle (n=6 from each group).

Statistical Analysis

Numerical values are expressed as mean±SEM unless otherwise indicated. Comparisons of parameters between 2 groups were made with unpaired Student t test. Comparisons of parameters among 3 groups were made with a 1-way ANOVA, followed by the Scheffe multiple-comparison test. Comparisons of changes in parameters among the 3 groups were made by a 2-way ANOVA for repeated measures, followed by the Scheffe multiple-comparison test. A value of $P<0.05$ was considered significant.

Results

Characterization of Cultured MSCs

Most cultured MSCs expressed CD29 and CD90 (Figure 1). In contrast, the majority of MSCs were negative for CD31, CD34, CD45, and SMA. Some of the MSCs expressed c-Kit and vimentin.

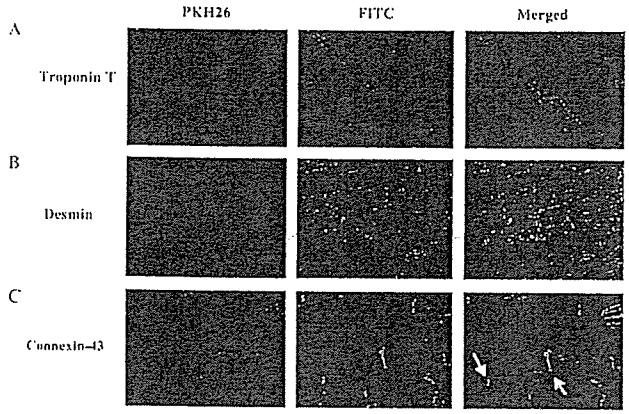

Figure 2. Differentiation of transplanted MSCs into cardiomyocytes. Transplanted MSCs were engrafted in the myocardium and stained for cardiac troponin T (A) and desmin (B). Engrafted MSCs also expressed connexin-43, a gap junction protein, at contact points with native cardiac myocytes (left arrow) and other transplanted cells (right arrow) (C). Magnification ×400.

Myogenesis and Angiogenesis Induced by MSCs

Red fluorescence–labeled MSCs were transplanted into the myocardium 5 weeks after immunization. Four weeks after transplantation, MSCs were engrafted into the myocardium (Figure 2). Immunofluorescence demonstrated that transplanted MSCs were positive for the cardiac markers cardiac troponin T and desmin (Figure 2). Transplanted MSCs also expressed connexin-43, a gap junction protein, at contact points with native cardiac myocytes as well as with MSCs. FACS analysis of isolated heart cells demonstrated that 8±1% of transplanted MSCs were double-positive for PKH26 and troponin T. These results suggest that a small number of transplanted MSCs can differentiate into cardiomyocytes.

Some transplanted MSCs formed vascular structures in the myocardium and were positive for von Willebrand factor (Figure 3A). Other MSCs were positive for SMA and participated in vessel formation as mural cells (Figure 3B). Alkaline phosphatase staining of the ischemic myocardium showed marked augmentation of neovascularization in the MSC-treated DCM group (Figures 4A–4C). Quantitative analysis demonstrated that capillary density was significantly

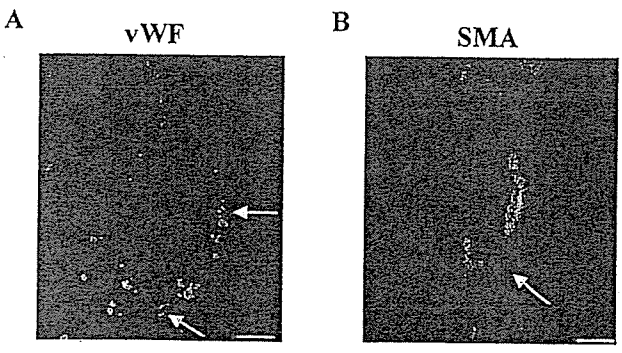

Figure 3. Differentiation of transplanted MSCs into vascular endothelial cells and smooth muscle cells. Some of the transplanted MSCs were positive for von Willebrand factor (vWF, A) and SMA (B) and formed vascular structures (A and B). Scale

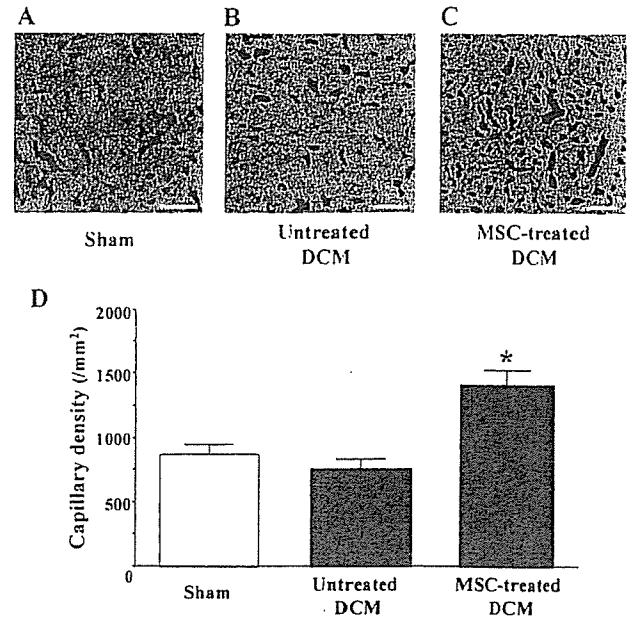

Figure 4. A–C, Representative samples of alkaline phosphatase staining of myocardium. Magnification, ×200. Scale bars=10 μm. D, Quantitative analysis of capillary density in the myocardium. Data are mean±SEM *P<0.05 vs untreated DCM group.

higher in the MSC-treated DCM group than in the untreated DCM group (Figure 4D).

Angiogenic, Antiapoptotic, and Mitogenic Factors Released From MSCs

After 24 hours of culture, MSCs secreted large amounts of angiogenic and antiapoptotic factors, including VEGF, HGF, and AM (Figure 5). Compared with MNCs that have commonly been used for regenerative therapy,[20–22] MSCs secreted 4-fold more VEGF and 5-fold more HGF. Similarly, MSCs secreted 6-fold more AM, an angiogenic and antiapoptotic peptide, compared with MNCs. MSCs also secreted a large amount, 10-fold greater than MNCs, of IGF-1, a growth hormone mediator for myocardial growth (Figure 5). Transplantation of MSCs significantly increased circulating VEGF (45.8±1.6 to 68.5±3.6 pg/mL, P<0.05), HGF (431.8±56.6 to 517.2±67.1 pg/mL, P<0.05), and AM (23.4±0.8 to 41.2±4.8 pg/mL, P<0.05) 24 hours after transplantation, although vehicle injection did not alter these parameters. Serum IGF-1 tended to increase after MSC transplantation (938.1±151.6 to 1063.5±116.9 pg/mL, P=NS), but this increase did not reach statistical significance.

Hemodynamic Effects of MSC Transplantation

Nine weeks after immunization, LV end-diastolic pressure showed a marked elevation in the untreated DCM group; this elevation was significantly attenuated in the MSC-treated DCM group (Figure 6A). LV maximum *dP/dt* was significantly lower in the untreated DCM group than in the sham group (Figure 6B). However, LV maximum *dP/dt* was significantly improved 4 weeks after MSC transplantation. There was no significant difference in heart rate or mean arterial pressure among the 3 groups (the Table). Echocar-

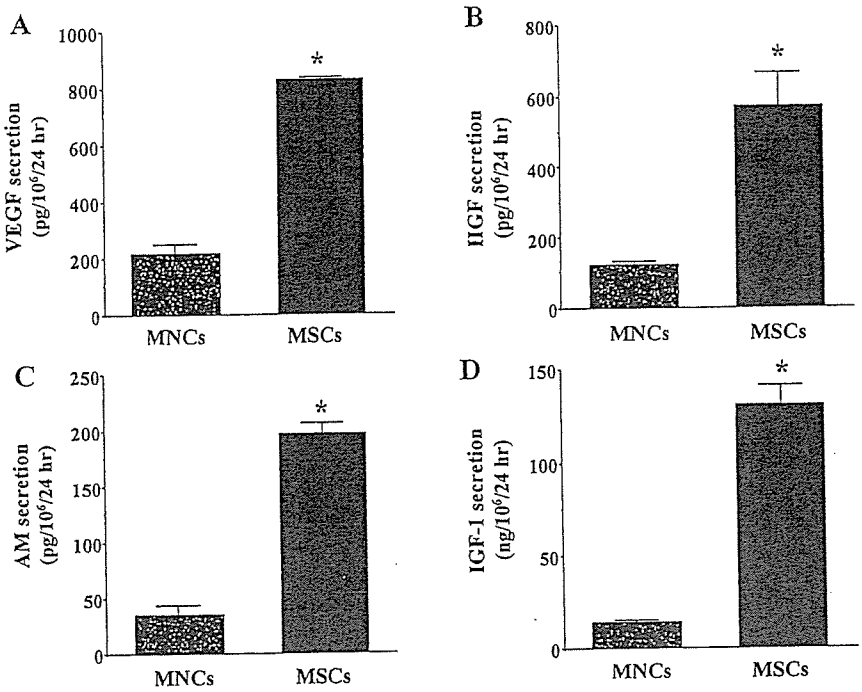

Figure 5. A–D, Angiogenic, antiapoptotic, and mitogenic factors produced by MSCs and bone marrow–derived MNCs). Compared with MNCs, MSCs secreted large amounts of VEGF, HGF, AM, and IGF-1. *$P<0.05$ vs MNCs.

in the untreated DCM group, as indicated by a decrease in percent fractional shortening and an increase in LV diastolic dimension (Figure 6C and 6D). However, MSC transplantation increased percent fractional shortening and inhibited the increase in LV diastolic dimension.

Reduction of Myocardial Fibrosis by MSC Transplantation

Masson's trichrome staining demonstrated modest myocardial fibrosis in the untreated DCM group (Figure 7A). However, MSC transplantation significantly attenuated the development of myocardial fibrosis. Quantitative analysis also demonstrated that the collagen volume fraction in the MSC-treated DCM group was significantly smaller than that in the untreated DCM group (Figure 7B). Western blot analysis showed that myocardial contents of MMP-2 and MMP-9 in the untreated DCM were significantly increased compared with those in the sham group (Figure 7C–E). However, the increases in MMP-2 and MMP-9 levels were attenuated by MSC transplantation, although the change in MMP-9 did not reach statistical significance.

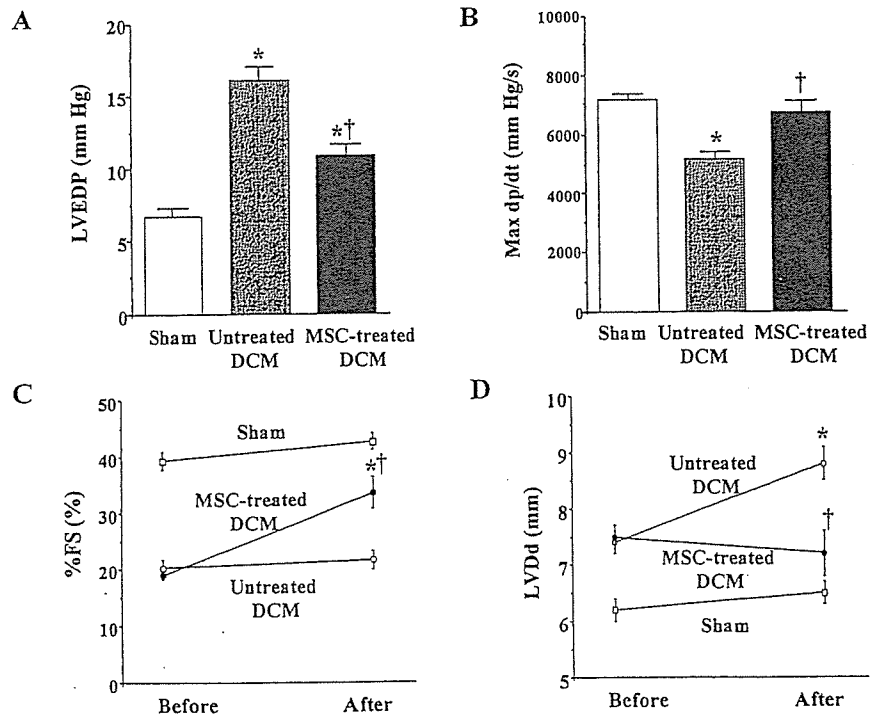

Figure 6. A and B, Effects of MSC transplantation on hemodynamic parameters. LVEDP indicates LV end-diastolic pressure; Max *dP/dt*, LV maximum *dP/dt*. Data are mean±SEM. *$P<0.05$ vs sham group; †$P<0.05$ vs untreated DCM group. C and D, Changes in echocardiographic parameters induced by MSC transplantation. %FS indicates LV fractional shortening. Data are mean±SEM *$P<0.05$ vs before transplantation; †$P<0.05$ vs the time-matched untreated DCM group.

Physiological Profiles of the 3 Experimental Groups

	Sham	Untreated DCM	MSC-Treated DCM
n	10	10	10
Body wt, g	421±8	372±4*	389±5*
LV wt/body wt, g/kg	1.91±0.05	2.18±0.06*	2.05±0.05
RV wt/body wt, g/kg	0.55±0.01	0.68±0.02*	0.60±0.03†
Heart rate, bpm	403±10	432±15	417±12
Mean arterial pressure, mm Hg	134±2	123±3	132±5

wt indicates weight; RV, right ventricle. Sham-operated rats were given vehicle only. The untreated DCM group included DCM rats treated with vehicle. The MSC-treated DCM group included DCM rats treated with MSCs. Data are mean±SEM.

*P<0.05 vs sham group; †P<0.05 vs untreated DCM group.

Discussion

In the present study, we have demonstrated the following effects of MSC transplantation in a rat model of DCM: (1) induction of myogenesis and angiogenesis; (2) differentiation of transplanted MSCs into cardiomyocytes, vascular endothelial cells, and smooth muscle cells; (3) secretion of large amounts of VEGF, HGF, AM, and IGF-1; (4) improvement of cardiac function and inhibition of ventricular remodeling; and (5) decrease in collagen volume fraction in the myocardium.

Earlier studies have shown that transplantation of MSCs improves cardiac function in experimental models of ischemic heart disease.[9,23] However, little information is available about the therapeutic potential of MSCs for chronic heart failure due to DCM. Previous studies have shown that porcine cardiac myosin-induced myocarditis progresses to a chronic phase resembling DCM.[13,14] Thus, we used this model 5 weeks after immunization as an example of experimental DCM.

In the present study, transplanted MSCs were engrafted into the myocardium in a rat model of DCM. Four weeks after transplantation, some of the engrafted MSCs were positively stained for cardiac troponin T and desmin. Transplanted MSCs also expressed connexin-43, a gap junction protein, at contact points with native cardiac myocytes as well as with MSCs. These results suggest that MSCs differentiate into cardiomyocytes in the myocardium and form connections with native cardiomyocytes in rats with DCM. Unlike earlier studies that have used a model of myocardial infarction,[7,9,23] we used a rat model of DCM to demonstrate the engraftment and cardiogenic differentiation of MSCs. Importantly, MSC transplantation improved cardiac function in these rats, as indicated by a significant decrease in LV end-diastolic pressure and an increase in LV dP/dt_{max}. Thus, the improvement in cardiac function may be a result of MSC-induced myocardial regeneration; however, further studies are necessary to investigate the mechanisms by which MSCs develop into cardiac myocyte–like cells.

Some of the transplanted MSCs were positive for a vascular endothelial cell marker and participated in vessel formation. MSC transplantation significantly increased capillary density in the myocardium. SMA staining revealed that MSCs differentiated into vascular smooth muscle cells, which play an important role in vessel maturation. Earlier studies have shown that transplantation of MNCs induces therapeutic angiogenesis in patients with limb ischemia or ischemic heart disease.[20–22] The angiogenic potential of MNCs is mediated at least in part by production by the cells of a variety of angiogenic factors.[24] Although MSCs have also been shown to produce VEGF,[10,25] there has been no study to compare their production between MSCs and MNCs. The present study demonstrated that MSCs secreted ≈4-fold more VEGF compared with MNCs. Furthermore, MSCs secreted large amounts of HGF and AM, potent angiogenic factors.[26–30] Taking these findings together, MSCs may contribute to neovascularization in the myocardium not only through their ability to generate capillary-like structures but also through growth factor–mediated paracrine regulation. Myocardial blood flow abnormalities have been documented in patients with heart failure caused by DCM.[12] Thus, it is possible that MSC-induced neovascularization contributes to improvement in cardiac function.

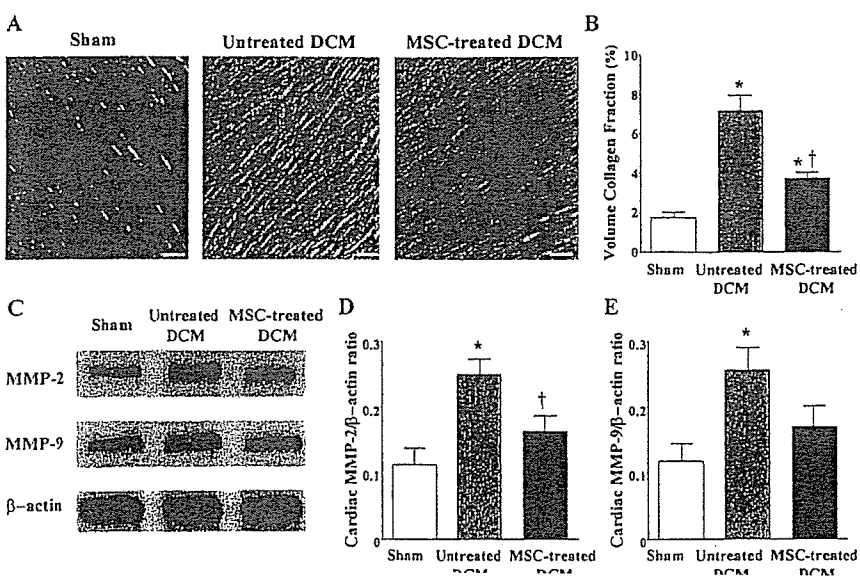

Figure 7. Effects of MSC transplantation on myocardial fibrosis. A, Photomicrographs show representative myocardial sections stained with Masson's trichrome. Scale bars=10 μm. B, Quantitative analysis demonstrated that the collagen volume fraction in the MSC-treated DCM group was significantly smaller than that in the untreated DCM group. C, Representative Western blots for MMPs-2 and -9 and β-actin in the heart. D and E, Quantitative analysis of cardiac tissue contents of MMP-2 and -9. Data are mean±SEM *P<0.05 vs sham group; †P<0.05 vs untreated DCM group.

HGF has not only angiogenic but also cardioprotective effects, including antiapoptotic, mitogenic, and antifibrotic activities.[26,27] *HGF* gene transfer into the myocardium improves myocardial function and geometry.[28] In particular, the antifibrotic effects of HGF through inhibition of transforming growth factor-β expression is beneficial for heart failure. Cultured MSCs secreted a large amount of HGF. In vivo, transplantation of MSCs slightly increased plasma HGF in rats. It significantly attenuated the development of myocardial fibrosis in a rat model of DCM. These results suggest that MSC-derived HGF may contribute to improvements in cardiac function partly through its antifibrotic effects.

MSCs also produced AM, a potent vasodilator and cardioprotective peptide.[29] We have shown that AM prevents cardiomyocyte apoptosis through the phosphatidylinositol 3-kinase/Akt–dependent pathway[16] and that it has potent angiogenic effects.[30] AM inhibits proliferation of cardiac fibroblasts through the cAMP-dependent pathway.[31] Administration of AM inhibits LV remodeling and improves cardiac function in heart failure.[32–34] In the present study, cultured MSCs secreted a large amount of AM in vitro. In vivo, transplantation of MSCs markedly increased plasma AM level. Taken together, these findings suggest that MSCs may exert their cardioprotective effects through AM-mediated paracrine regulation.

IGF-1, a growth hormone mediator, plays an important role in myocardial and skeletal muscle growth.[35,36] Administration of IGF-1 improves cardiac function after myocardial infarction through enhancement of myocardial growth.[37] Its protective and antiapoptotic properties have been demonstrated in different models of myocardial ischemia.[38] Furthermore, IGF-1 exerts Ca^{2+}-dependent, positive inotropic effects through a phosphatidylinositol 3-kinase–dependent pathway.[39] Interestingly, the present study demonstrated that MSCs secreted significant amounts of IGF-1 in vitro, 10-fold greater than MNCs. These findings raise the possibility that MSC-derived IGF-1 may participate in myocardial growth and enhancement of myocardial contractility in a rat model of DCM.

MMPs also play a crucial role in extracellular remodeling in heart failure.[40] In fact, pharmacological inhibition of MMP activities prevents progressive LV remodeling in an animal model of heart failure.[41] In the present study, cardiac MMP-2 and MMP-9 were increased in rats with DCM, which is consistent with recent findings in patients with heart failure.[40,42] Interestingly, MSC transplantation attenuated the increases in cardiac MMP-2 and MMP-9 in a rat model of DCM. Although the underlying mechanisms remain unclear, MSC transplantation may influence extracellular remodeling in heart failure.

The present study has some limitations. First, immunohistochemical evidence suggests differentiation of MSCs into cardiomyocytes, vascular endothelial cells, and smooth muscle cells. However, further studies are necessary to convincingly demonstrate differentiation of MSCs into a specific cell type. Second, the model of DCM used in this study was an injury model, and the effects of treatment may be related to attenuation of the injury rather than to the established cardiomyopathy. Nonetheless, the experiment was performed 5 to 9 weeks after myosin injection, by which time inflammatory changes were hardly observed and had been replaced by fibrosis.[43]

Conclusions

MSC transplantation improved cardiac function in a rat model of DCM, possibly through induction of myogenesis and angiogenesis, as well as by inhibition of myocardial fibrosis. The beneficial effects of MSCs may be mediated at least in part by their differentiation into cardiomyocytes and vascular cells and by their ability to supply large amounts of angiogenic, antiapoptotic, and mitogenic factors. Thus, MSC transplantation has potential as a new therapeutic strategy for the treatment of DCM.

Acknowledgments

This work was supported by research grants for cardiovascular disease (16C-6) and Human Genome Tissue Engineering 009 from the Ministry of Health, Labor and Welfare; the Industrial Technology Research Grant Program in '03 from the New Energy and Industrial Technology Development Organization of Japan; a research grant from the Japan Cardiovascular Research Foundation; and Promotion of Fundamental Studies in Health Science of the Organization for Pharmaceutical Safety and Research of Japan.

References

1. Cohn JN. The management of chronic heart failure. *N Engl J Med.* 1996;335:490–498.
2. Dec GW, Fuster V. Idiopathic dilated cardiomyopathy. *N Engl J Med.* 1994;331:1564–1575.
3. Beltrami AP, Urbanek K, Kajstura J, Yan SM, Finato N, Bussani R, Nadal-Ginard B, Silvestri F, Leri A, Beltrami CA, Anversa P. Evidence that human cardiac myocytes divide after myocardial infarction. *N Engl J Med.* 2001;344:1750–1757.
4. Pittenger MF, Mackay AM, Beck SC, Jaiswal RK, Douglas R, Mosca JD, Moorman MA, Simonetti DW, Craig S, Marshak DR. Multilineage potential of adult human mesenchymal stem cells. *Science.* 1999;284:143–147.
5. Reyes M, Dudek A, Jahagirdar B, Koodie L, Marker PH, Verfaillie CM. Origin of endothelial progenitors in human postnatal bone marrow. *J Clin Invest.* 2002;109:337–346.
6. Toma C, Pittenger MF, Cahill KS, Byrne BJ, Kessler PD. Human mesenchymal stem cells differentiate to a cardiomyocyte phenotype in the adult murine heart. *Circulation.* 2002;105:93–98.
7. Mangi AA, Noiseux N, Kong D, He H, Rezvani M, Ingwall JS, Dzau VJ. Mesenchymal stem cells modified with Akt prevent remodeling and restore performance of infarcted hearts. *Nat Med.* 2003;9:1195–1201.
8. Makino S, Fukuda K, Miyoshi S, Konishi F, Kodama H, Pan J, Sano M, Takahashi T, Hori S, Abe H, Hata J, Umezawa A, Ogawa S. Cardiomyocytes can be generated from marrow stromal cells in vitro. *J Clin Invest.* 1999;103:697–705.
9. Shake JG, Gruber PJ, Baumgartner WA, Senechal G, Meyers J, Redmond JM, Pittenger MF, Martin BJ. Mesenchymal stem cell implantation in a swine myocardial infarct model: engraftment and functional effects. *Ann Thorac Surg.* 2002;73:1919–1925.
10. Al-Khaldi A, Al-Sabti H, Galipeau J, Lachapelle K. Therapeutic angiogenesis using autologous bone marrow stromal cells: improved blood flow in a chronic limb ischemia model. *Ann Thorac Surg.* 2003;75:204–209.
11. Al-Khaldi A, Eliopoulos N, Martineau D, Lejeune L, Lachapelle K, Galipeau J. Postnatal bone marrow stromal cells elicit a potent VEGF-dependent neoangiogenic response in vivo. *Gene Ther.* 2003;10:621–629.
12. Parodi O, De Maria R, Oltrona L, Testa R, Sambuceti G, Roghi A, Merli M, Belingheri L, Accinni R, Spinelli F, Pellegrini A, Baroldi G. Myocardial blood flow distribution in patients with ischemic heart disease or dilated cardiomyopathy undergoing heart transplantation. *Circulation.* 1993;88:509–522.
13. Kodama M, Zhang S, Hanawa H, Saeki M, Inomata T, Suzuki K, Koyama S, Shibata A. Effects of 15-deoxyspergualin on experimental autoimmune giant cell myocarditis of the rat. *Circulation.* 1995;91:1116–1122.
14. Watanabe K, Ohta Y, Nakazawa M, Higuchi H, Hasegawa G, Naito M, Fuse K, Ito M, Hirono S, Tanabe N, Hanawa H, Kato K, Kodama M, Aizawa Y. Low dose carvedilol inhibits progression of heart failure in rats with dilated cardiomyopathy. *Br J Pharmacol.* 2000;130:1489–1495.

15. Nagaya N, Uematsu M, Kojima M, Ikeda Y, Yoshihara F, Shimizu W, Hosoda H, Hirota Y, Ishida H, Mori H, Kangawa K. Chronic administration of ghrelin improves left ventricular dysfunction and attenuates development of cardiac cachexia in rats with heart failure. *Circulation*. 2001;104:1430–1435.
16. Okumura H, Nagaya N, Itoh T, Okano I, Hino J, Mori K, Tsukamoto Y, Ishibashi-Ueda H, Miwa S, Tambara K, Toyokuni S, Yutani C, Kangawa K. Adrenomedullin infusion attenuates myocardial ischemia/reperfusion injury through the phosphatidylinositol 3-kinase/Akt-dependent pathway. *Circulation*. 2004:109:242–248.
17. Messina LM, Podrazik RM, Whitehill TA, Ekhterae D, Brothers TE, Wilson JM, Burkel WE, Stanley JC. Adhesion and incorporation of lacZ-transduced endothelial cells into the intact capillary wall in the rat. *Proc Natl Acad Sci U S A*. 1992;89:12018–12022.
18. Harada M, Itoh H, Nakagawa O, Ogawa Y, Miyamoto Y, Kuwahara K, Ogawa E, Igaki T, Yamashita J, Masuda I, Yoshimasa T, Tanaka I, Saito Y, Nakao K. Significance of ventricular myocytes and nonmyocytes interaction during cardiocyte hypertrophy: evidence for endothelin-1 as a paracrine hypertrophic factor from cardiac nonmyocytes. *Circulation*. 1997;96:3737–3744.
19. Ohta H, Tsuji T, Asai S, Sasakura K, Teraoka H, Kitamura K, Kangawa K. A simple immunoradiometric assay for measuring the entire molecules of adrenomedullin in human plasma. *Clin Chim Acta*. 1999;287:B131–B143.
20. Murohara T, Ikeda H, Duan J, Shintani S, Sasaki K, Eguchi H, Onitsuka I, Matsui K, Imaizumi T. Transplanted cord blood-derived endothelial precursor cells augment postnatal neovascularization. *J Clin Invest*. 2000; 105:1527–1536.
21. Tateishi-Yuyama E, Matsubara H, Murohara T, Ikeda U, Shintani S, Masaki H, Amano K, Kishimoto Y, Yoshimoto K, Akashi H, Shimada K, Iwasaka T, Imaizumi T. Therapeutic Angiogenesis using Cell Transplantation (TACT) Study Investigators. Therapeutic angiogenesis for patients with limb ischaemia by autologous transplantation of bone-marrow cells: a pilot study and a randomised controlled trial. *Lancet*. 2002;360:427–435.
22. Tse HF, Kwong YL, Chan JK, Lo G, Ho CL, Lau CP. Angiogenesis in ischaemic myocardium by intramyocardial autologous bone marrow mononuclear cell implantation. *Lancet*. 2003;4:47–49.
23. Min JY, Sullivan MF, Yang Y, Zhang JP, Converso KL, Morgan JP, Xiao YF. Significant improvement of heart function by cotransplantation of human mesenchymal stem cells and fetal cardiomyocytes in postinfarcted pigs. *Ann Thorac Surg*. 2002;74:1568–1575.
24. Kamihata H, Matsubara H, Nishiue T, Fujiyama S, Tsutsumi Y, Ozono R, Masaki H, Mori Y, Iba O, Tateishi E, Kosaki A, Shintani S, Murohara T, Imaizumi T, Iwasaka T. Implantation of bone marrow mononuclear cells into ischemic myocardium enhances collateral perfusion and regional function via side supply of angioblasts, angiogenic ligands, and cytokines. *Circulation*. 2001;104:1046–1052.
25. Kinnaird T, Stabile E, Burnett MS, Lee CW, Barr S, Fuchs S, Epstein SE. Marrow-derived stromal cells express genes encoding a broad spectrum of arteriogenic cytokines and promote in vitro and in vivo arteriogenesis through paracrine mechanisms. *Circ Res*. 2004;94:678–685.
26. Nakamura T, Nishizawa T, Hagiya M, Seki T, Shimonishi M, Sugimura A, Tashiro K, Shimizu S. Molecular cloning and expression of human hepatocyte growth factor. *Nature*. 1989;342:440–443.
27. Nakamura T, Mizuno S, Matsumoto K, Sawa Y, Matsuda H, Nakamura T. Myocardial protection from ischemia/reperfusion injury by endogenous and exogenous HGF. *J Clin Invest*. 2000;106:1511–1519.
28. Li Y, Takemura G, Kosai K, Yuge K, Nagano S, Esaki M, Goto K, Takahashi T, Hayakawa K, Koda M, Kawase Y, Maruyama R, Okada H, Minatoguchi S, Mizuguchi H, Fujiwara T, Fujiwara H. Postinfarction treatment with an adenoviral vector expressing hepatocyte growth factor relieves chronic left ventricular remodeling and dysfunction in mice. *Circulation*. 2003;107:2499–2506.
29. Kitamura K, Kangawa K, Kawamoto M, Ichiki Y, Nakamura S, Matsuo H, Eto T. Adrenomedullin: a novel hypotensive peptide isolated from human pheochromocytoma. *Biochem Biophys Res Commun*. 1993;192:553–560.
30. Tokunaga N, Nagaya N, Shirai M, Tanaka E, Ishibashi-Ueda H, Harada-Shiba M, Kanda M, Ito T, Shimizu W, Tabata Y, Uematsu M, Nishigami K, Sano S, Kangawa K, Mori H. Adrenomedullin gene transfer induces therapeutic angiogenesis in a rabbit model of chronic hind limb ischemia: benefits of a novel nonviral vector, gelatin. *Circulation*. 2004;109:526–531.
31. Tsuruda T, Kato J, Kitamura K, Kawamoto M, Kuwasako K, Imamura T, Koiwaya Y, Tsuji T, Kangawa K, Eto T. An autocrine or a paracrine role of adrenomedullin in modulating cardiac fibroblast growth. *Cardiovasc Res*. 1999;43:958–967.
32. Nishikimi T, Yoshihara F, Horinaka S, Kobayashi N, Mori Y, Tadokoro K, Akimoto K, Minamino N, Kangawa K, Matsuoka H. Chronic administration of adrenomedullin attenuates transition from left ventricular hypertrophy to heart failure in rats. *Hypertension*. 2003;42:1034–1041.
33. Nakamura R, Kato J, Kitamura K, Onitsuka H, Imamura T, Cao Y, Marutsuka K, Asada Y, Kangawa K, Eto T. Adrenomedullin administration immediately after myocardial infarction ameliorates progression of heart failure in rats. *Circulation*. 2004;110:426–431.
34. Nagaya N, Satoh T, Nishikimi T, Uematsu M, Furuichi S, Sakamaki F, Oya H, Kyotani S, Nakanishi N, Goto Y, Masuda Y, Miyatake K, Kangawa K. Hemodynamic, renal, and hormonal effects of adrenomedullin infusion in patients with congestive heart failure. *Circulation*. 2000;101:498–503.
35. Fuller J, Mynett JR, Sugden PH. Stimulation of cardiac protein synthesis by insulin-like growth factors. *Biochem J*. 1992;282:85–90.
36. Florini JR, Ewton DZ, Coolican SA. Growth hormone and the insulin-like growth factor system in myogenesis. *Endocr Rev*. 1996;17:481–517.
37. Cittadini A, Stromer H, Katz SE, Clark R, Moses AC, Morgan JP, Douglas PS. Differential cardiac effects of growth hormone and insulin-like growth factor-1 in the rat: a combined in vivo and in vitro evaluation. *Circulation*. 1996;93:800–809.
38. Li Q, Li B, Wang X, Leri A, Jana KP, Liu Y, Kajstura J, Baserga R, Anversa P. Overexpression of insulin-like growth factor-1 in mice protects from myocyte death after infarction, attenuating ventricular dilation, wall stress, and cardiac hypertrophy. *J Clin Invest*. 1997;100:1991–1999.
39. von Lewinski D, Voss K, Hulsmann S, Kogler H, Pieske B. Insulin-like growth factor-1 exerts Ca^{2+}-dependent positive inotropic effects in failing human myocardium. *Circ Res*. 2003;92:169–176.
40. Thomas CV, Coker ML, Zellner JL, Handy JR, Crumbley AJ 3rd, Spinale FG. Increased matrix metalloproteinase activity and selective upregulation in LV myocardium from patients with end-stage dilated cardiomyopathy. *Circulation*. 1998;97:1708–1715.
41. Spinale FG, Coker ML, Krombach SR, Mukherjee R, Hallak H, Houck WV, Clair MJ, Kribbs SB, Johnson LL, Peterson JT, Zile MR. Matrix metalloproteinase inhibition during the development of congestive heart failure: effects on left ventricular dimensions and function. *Circ Res*. 1999;85:364–376.
42. Spinale FG, Coker ML, Heung LJ, Bond BR, Gunasinghe HR, Etoh T, Goldberg AT, Zellner JL, Crumbley AJ. A matrix metalloproteinase induction/activation system exists in the human left ventricular myocardium and is upregulated in heart failure. *Circulation*. 2000;102:1944–1949.
43. Kodama M, Matsumoto Y, Fujiwara M, Zhang SS, Hanawa H, Itoh E, Tsuda T, Izumi T, Shibata A. Characteristics of giant cells and factors related to the formation of giant cells in myocarditis. *Circ Res*. 1991;69:1042–1050.

CLINICAL PERSPECTIVE

Transplantation of stem or progenitor cells has the potential to improve and restore cardiac function. To date, experimenters investigating the possible therapeutic effects of stem cells in the heart have used models of infarction, and little information is available about the therapeutic potential of cell transplantation for heart failure due to dilated cardiomyopathy. In the present study, we demonstrated that transplantation of stem cells improved cardiac function in a model of myocarditis. We found evidence that stem cells may work to improve heart function by both myogenesis and angiogenesis while inhibiting myocardial fibrosis. Based on our data, part of the mechanism for this improvement may occur through the action of stem cells as a source of growth factors and cytokines in the heart. This study supports the overall notion that mesenchymal stem cells transplanted into the failing heart have potential as a new therapeutic strategy for the treatment of dilated cardiomyopathy.

Invited Review

Am J Physiol Regul Integr Comp Physiol 288: R1432–R1437, 2005;
doi:10.1152/ajpregu.00662.2004.

Adrenomedullin: angiogenesis and gene therapy

Noritoshi Nagaya,[1,2] Hidezo Mori,[3] Shinsuke Murakami,[1] Kenji Kangawa,[4] and Soichiro Kitamura[5]

[1]Department of Regenerative Medicine and Tissue Engineering, [2]Department of Internal Medicine, [3]Department of Cardiac Physiology, [4]Department of Biochemistry, [5]Department of Cardiovascular Surgery, National Cardiovascular Center Research Institute, Osaka, Japan

Nagaya, Noritoshi, Hidezo Mori, Shinsuke Murakami, Kenji Kangawa, and Soichiro Kitamura. Adrenomedullin: angiogenesis and gene therapy. *Am J Physiol Regul Integr Comp Physiol* 288: R1432–R1437, 2005; doi:10.1152/ajpregu.00662.2004.—Adrenomedullin (AM) is a potent, long-lasting vasodilator peptide that was originally isolated from human pheochromocytoma. AM signaling is of particular significance in endothelial cell biology since the peptide protects cells from apoptosis, promotes angiogenesis, and affects vascular tone and permeability. The angiogenic effect of AM is mediated by activation of Akt, mitogen-activated protein kinase/extracellular signal-regulated kinase 1/2, and focal adhesion kinase in endothelial cells. Both AM and its receptor, calcitonin receptor-like receptor, are upregulated through a hypoxia-inducible factor-1-dependent pathway under hypoxic conditions. Thus AM signaling plays an important role in the regulation of angiogenesis in hypoxic conditions. Recently, we have developed a nonviral vector, gelatin. Positively charged gelatin holds negatively charged plasmid DNA in its lattice structure. DNA-gelatin complexes can delay gene degradation, leading to efficient gene transfer. Administration of AM DNA-gelatin complexes induces potent angiogenic effects in a rabbit model of hindlimb ischemia. Thus gelatin-mediated AM gene transfer may be a new therapeutic strategy for the treatment of tissue ischemia. Endothelial progenitor cells (EPCs) play an important role in endothelial regeneration. Interestingly, EPCs phagocytose ionically linked DNA-gelatin complexes in coculture, which allows nonviral gene transfer into EPCs. AM gene transfer into EPCs inhibits cell apoptosis and induces proliferation and migration, suggesting that AM gene transfer strengthens the therapeutic potential of EPCs. Intravenous administration of AM gene-modified EPCs regenerate pulmonary endothelium, resulting in improvement of pulmonary hypertension. These results suggest that in vivo and in vitro transfer of AM gene using gelatin may be applicable for intractable cardiovascular disease.

regeneration; endothelium; ischemia; pulmonary hypertension

ADRENOMEDULLIN (AM) IS A POTENT, long-lasting vasodilator peptide that was originally isolated from human pheochromocytoma (36). The peptide consists of 52 amino acids with an intramolecular disulfide bond, sharing slight homology with calcitonin gene-related peptide and amylin. Immunoreactive AM is detected in plasma and a variety of tissues including, blood vessels, heart, and lungs (19). Particularly, AM shows a variety of effects on the vasculature that include vasodilatation (23), regulation of permeability (16), inhibition of endothelial apoptosis (31), and promotion of angiogenesis (1, 35, 60). In addition, AM has protective effects against vascular injury, including oxidative stress (33, 69, 84). It is becoming clear that either activation or disruption of AM signaling might contribute to many pathological conditions, including hypertension (22), congestive heart failure (55), pulmonary hypertension (29), neoplastic growth (39), and inflammatory disease (59). To date, the major biological acitivities of AM in vitro and in vivo are *1)* vasodilation, *2)* diuresis and natriuresis, *3)* positive inotropic effect, *4)* inhibition of endothelial cell apoptosis, *5)* induction of angiogenesis, *6)* inhibition of cardiomyocyte apoptosis, *7)* suppression of aldosterone production, *8)* anti-inflammatory activity, and *9)* antioxidant activity. We and others have demonstrated that intravenous administration of AM decreases systemic and pulmonary arterial pressure and induces diuresis and natriuresis (47, 52, 65), suggesting that AM is involved in the regulation of vascular tone and body fluid. Subsequent studies have demonstrated beneficial hemodynamic effects and direct cardioprotective effects of AM infusion in the treatment of congestive heart failure (57, 61–64).

Until recently, only vascular endothelial growth factor (VEGF) (80), fibroblast growth factor (68), platelet-derived growth factor (37), and angiopoietin (74) were known to have profound angiogenic effects. More recently, however, the angiogenic potential of AM has attracted investigators' attention (35, 41, 59, 81). A previous study has shown that vascular abnormalities are present in homozygous AM knockout mice (70), suggesting that AM is essential for vascular morphogenesis. AM activates the PI3K/Akt-dependent pathway in vascular endothelial cells (58), which is considered to regulate multiple critical steps in angiogenesis, including endothelial cell survival, proliferation, migration, and capillary-like structure formation (27). These findings raise the possibility that AM plays a role in modulating angiogenesis and neovascular-

Address for reprint requests and other correspondence: Noritoshi Nagaya, Dept. of Regenerative Medicine and Tissue Engineering, National Cardiovascular Center Research Institute, 5-7-1 Fujishirodai, Suita, Osaka 565-8565, Japan (E-mail: nnagaya@ri.ncvc.go.jp).

ization. This review focused on the angiogenic effects of AM and the therapeutic potential of AM gene transfer for the treatment of intractable cardiovascular disease.

ENDOGENOUS AM PRODUCTION IN ISCHEMIC CONDITIONS

Hypoxia (14, 53) and cytokine production (73) in ischemic heart disease or septic shock, as well as shear stress (7) in hypertension and heart failure induce AM secretion by vascular cells (Fig. 1). We have shown that plasma AM level is increased in patients with acute myocardial infarction (40, 49), peripheral arterial occlusive disease (75), and congestive heart failure (28, 55). Tissue levels of AM peptide and mRNA are also markedly increased in ischemic myocardium (18, 50) and failing heart (8, 56, 78, 82). These findings suggest that expression of AM is upregulated under tissue ischemia and inflammation, both of which are associated with neovascularization. An in vitro study has demonstrated that AM is upregulated through a hypoxia-inducible factor-1 (HIF-1)-dependent pathway under hypoxic conditions (14). Thus hypoxia/HIF-1 is one of the most potent regulators of AM production (Fig. 1). A recent study has demonstrated that heterozygous AM knockout mice [AM(+/−)] show significantly less blood flow recovery with less collateral capillary development than their wild-type mice (20). Administration of AM promotes blood flow recovery and capillary formation in AM(+/−) mice. These findings suggest that endogenous AM may play an important role in the regulation of angiogenesis under ischemic conditions. Considering the angiogenic potency of AM, increased endogenous AM represents a compensatory mechanism as an angiogenic factor promoting neovascularization under hypoxic conditions.

ANGIOGENIC EFFECTS OF AM AND ITS SIGNALING PATHWAY

AM signaling is of particular significance in endothelial cell biology since the peptide protects cells from apoptosis (31), promotes angiogenesis (35, 60), and affects vascular tone (23). Angiogenesis is a multistep process that involves migration and proliferation of endothelial cells, functional maturation of the newly assembled vessels, and remodeling of the extracellular matrix (26). Akt, mitogen-activated protein kinase (MAPK)/extracellular signal-regulated kinase 1/2 (ERK1/2), and focal adhesion kinase (p125FAK) play an important role in angiogenesis in endothelial cells. Kim et al. (35) demonstrated that AM activated Akt, MAPK/ERK1/2, and p125FAK in human umbilical vein endothelial cells (HUVECs), and produced increases in their DNA synthesis and migration. AM induced tube formation in HUVECs, and its effect was inhibited by pretreatment with a phosphatidylinositol 3′-kinase (PI3K) inhibitor or mitogen-activated protein kinase/extracellular signal-regulated kinase kinase (MEK)1/2 inhibitor. These findings suggest that AM exerts angiogenic activities through activation of Akt, MAPK, and p125FAK in endothelial cells (Fig. 1). In vivo, overexpression of AM augments collateral flow in ischemic tissues partly through activation of endothelial nitric oxide synthase (eNOS) (1). Earlier studies have shown that the vasodilatory effects of AM are mediated by cAMP/protein kinase in smooth muscle cells (SMCs) (23) and by the eNOS/NO pathway in endothelial cells (17). Thus AM-induced angiogenesis and vasodilation may synergistically improve blood perfusion in ischemic tissues.

Recently, a seven-transmembrane G-protein-coupled receptor, calcitonin receptor-like receptor (CRLR), and receptor activity modifying proteins (RAMPs) have been recognized as integral components of the AM signaling system (38, 43). CRLR has demonstrated the expression of the transcript predominantly in microvascular endothelial cells. This finding supports the view that CRLR is potentially a major mediator of the effects of AM on the vasculature. The effect of AM on CRLR is modified by RAMP2 and RAMP3. The angiogenic effect of AM is mediated by CRLR/RAMP2 and CRLR/RAMP3 receptors (Fig. 1). VEGF and AM act synergistically to induce angiogenic-related effects on endothelial cells in vitro (11). However, blocking antibodies to VEGF cannot significantly inhibit AM-induced capillary tube formation by

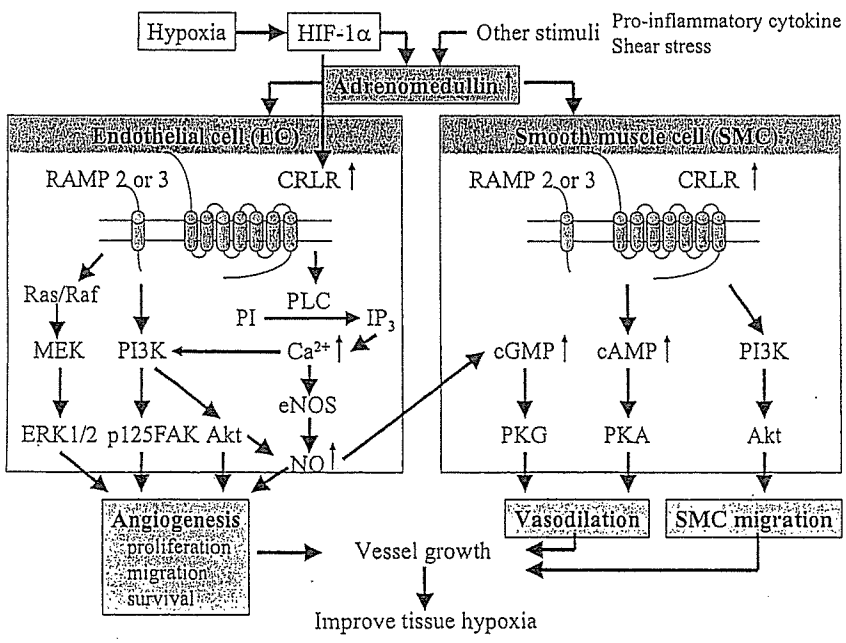

Fig. 1. Signaling pathway of adrenomedullin (AM) in vascular endothelial cells and smooth muscle cells. Both AM and calcitonin-receptor-like receptor (CRLR) are upregulated through a, hypoxia-inducible factor-1 (HIF-1)-dependent pathway under hypoxic conditions. AM binds to CRLR modified by receptor-activity-modifying protein 2 (RAMP2) and RAMP3. AM induces angiogenesis through activation of Akt, MAPK, and p125FAK in endothelial cells. AM also induces SMC migration and vasodilation. These activities synergistically improve tissue ischemia. MEK, mitogen-activated protein kinase/extracellular signal-regulated kinase kinase; ERK, extracellular signal-regulated kinase; PI3K, phosphatidylinositol 3-kinase; p125FAK, focal adhesion kinase; PLC, phospholipase C; PI, phosphatidylinositol; IP_3, inositol triphosphate; eNOS, endothelial nitric oxide synthase; NO, nitric oxide; cGMP, guanosine 3′,5′-cyclic monophosphate; PKG, protein kinase G; PKA, protein kinase A.

HUVECs, indicating that AM does not function indirectly through upregulation of VEGF. Interestingly, AM and CRLR are both upregulated under hypoxic conditions in microvascular endothelial cells, although expression of RAMPs is not activated by hypoxia in microvascular cells (54). The activity of the CRLR promoter under hypoxic conditions is regulated at least in part through hypoxia-responsive regulatory element binding transcription factor HIF-1. Thus the simultaneous transcriptional upregulation of CRLR and its ligand AM in endothelial cells might play a significant role in the vascular responses to hypoxia and ischemia by creating a potent survival loop.

SMCs are essential for the generation of functional and mature blood vessels (26). We demonstrated in vivo that intramuscular administration of AM increased the number of αSMA-positive cells involved in the formation of vascular structures (25). In vitro, AM enhanced SMC migration, which was inhibited by wortmannin, a PI3K inhibitor. Recent studies using homozygous AM knockout mice have suggested that AM is essential for vascular morphogenesis (6, 21, 70). Taking these findings together, it is possible that AM contributes to vessel maturation through enhancement of SMC migration via a PI3K/Akt-dependent pathway (Fig. 1). This feature of AM-induced angiogenesis is different from VEGF-induced angiogenesis, which is not associated with vessel muturation.

In tumor cells, inflammation and hypoxia increase AM expression, and the elevated expression of AM is associated with tumor neovascularization in xenografted endometrial tumors and renal cell carcinoma (12, 86). AM also acts as a tumor cell survival factor underlying human carcinogenesis. Thus hypoxia-induced AM plays a part in tumor angiogenesis in conjunction with VEGF, and facilitates tumor growth under hypoxic conditions. As angiogenesis is an essential process in tumor-host interactions for tumor growth, maintenance, and metastasis, finding ways to regulate the action of AM may provide a new avenue for developing anticancer therapy (16).

THERAPEUTIC ANGIOGENESIS

A variety of studies have demonstrated that AM gene delivery serves as therapeutic tool to protect the cardiovascular system, including the heart (9, 32, 85), kidney (83), and vasculature (2, 84). In this section, we describe the angiogenic potential of AM gene transfer using novel gene delivery systems:

Nonviral gene transfer. Peripheral vascular disease is a crucial health issue affecting an estimated 27 million people (5). Despite recent advances in medical interventions, the symptoms of some patients with critical limb ischemia fail to be controlled. Although gene therapy has been shown to be an effective approach for angiogenesis (10, 24, 72), it is still unsatisfactory because of the biohazard of viral vectors, low transfection efficiency, and premature tissue-targeting. Therefore, highly efficient and safe gene transfer is desirable. Recently, we developed a novel nonviral vector, gelatin hydrogel, which allows highly efficient and long-lasting gene transfer (13, 30, 81). Gelatin has been widely used as a carrier of protein because of its capacity to delay protein degradation (76, 77). Plasmid DNA is known to be negatively charged. Thus we used gelatin as a vector for gene therapy. Biodegradable gelatin was prepared from pig skin. The gelatin was characterized by a spheroid shape with a diameter of ~30 μm, water content of 95% and an isoelectric point of 9 after swelling in water (76, 77). After 2-h incubation, positively charged gelatin held negatively charged plasmid DNA in its positively charged lattice structure. DNA particles are released from the gelatin through its degradation. As a result, DNA-gelatin complexes can delay gene degradation, leading to efficient gene transfer (13, 30, 44, 81).

We examined whether nonviral vector gelatin-mediated AM gene transfer induces therapeutic angiogenesis in a rabbit model of hindlimb ischemia (81). Seven days after intramuscular injection of AM DNA-gelatin complexes, there was intense AM immunoreactivity surrounding the gelatin in the skeletal muscles. AM production in the AM-gelatin group was enhanced compared with that in the naked AM DNA group, which received plasmid AM DNA alone. Unlike AM production in the naked AM group, AM overexpression in the AM-gelatin group lasted for longer than 2 wk. Importantly, AM DNA-gelatin complexes induced more potent angiogenic effects in a rabbit model of hindlimb ischemia than naked AM DNA, as evidenced by significant increases in histological capillary density, calf blood pressure ratio, and laser Doppler flow. These results suggest that the use of biodegradable gelatin as a nonviral vector augments AM expression and enhances AM-induced angiogenic effects. AM DNA-gelatin complexes were distributed mainly in connective tissues. It is interesting to speculate that the delay of gene degradation by gelatin may have been responsible for the highly efficient gene transfer. Thus gelatin-mediated AM gene transfer may be a new therapeutic strategy for the treatment of severe peripheral vascular disease.

Cell-based gene transfer. Recently, transplantation of stem cells or progenitor cells has been shown to regenerate a variety of tissues. Endothelial progenitor cells (EPCs) have been discovered in adult peripheral blood (4, 79). EPCs are mobilized from bone marrow into the peripheral blood in response to tissue ischemia or traumatic injury, migrate to sites of injured endothelium, and differentiate into mature endothelial cells in situ (15, 34). Transplantation of EPC induces therapeutic angiogenesis in the ischemic heart or limb (34, 42, 71). However, some patients are refractory to conventional cell therapy because of insufficient cell number, poor survival, or impaired differentiation. Thus a novel therapeutic strategy to enhance the angiogenic properties of EPCs is desirable. Considering the variety of protective effects of AM on vascular endothelial cells, we hypothesized that AM gene transfer into EPCs would strengthen the therapeutic potential of EPCs. Genetically modified EPCs may serve not only as a tissue-engineering tool to reconstruct the vasculature but also as a vehicle for gene delivery to injured endothelium.

Here, we present a new concept for cell-based gene delivery into the vasculature, consisting of three processes (44). First, positively charged gelatin is readily complexed with negatively charged plasmid DNA. Second, EPCs phagocytose ionically linked plasmid DNA-gelatin complexes in coculture, which allows nonviral gene transfer into EPCs with high efficiency. Third, intravenously administered gene-modified EPCs are incorporated into injured vascular beds. This novel gene delivery system has great advantages over conventional gene therapy; it is nonviral and noninvasive, and it provides highly efficient gene targeting into the vasculature. These benefits

may be achieved mainly by the capability of EPCs to phagocytose DNA-gelatin complexes and to migrate to sites of injured endothelium. Genetically modified EPCs markedly secreted AM into the culture medium, and AM overproduction lasted for more than 2 wk. The proliferative activity of AM DNA-transduced EPCs exceeded that of nontransduced EPCs. Furthermore, AM gene transfer inhibited apoptosis of EPCs in vivo and in vitro. Thus ex vivo AM gene transfer strengthened the therapeutic potential of EPCs.

Primary pulmonary hypertension (PPH) is a rare, but life-threatening disease characterized by progressive pulmonary hypertension, ultimately producing right ventricular failure and death (67). Median survival in patients with PPH is considered to be 2.8 years from the time of diagnosis. Thus novel and effective therapy is needed for the treatment of pulmonary hypertension. Because endothelial dysfunction may play a role in the pathogenesis of pulmonary hypertension such as PPH (3), pulmonary endothelial cells may be a therapeutic target for the treatment of pulmonary hypertension. We have demonstrated that administration of AM peptide decreases pulmonary vascular resistance in patients with PPH (45, 46, 48, 51). Thus we investigated the effects of AM gene-modified EPCs on pulmonary hypertension in rats (44). AM gene-transduced EPCs were similarly incorporated into the pulmonary vasculature. Immunohistochemical analyses demonstrated that the transplanted EPCs were of endothelial lineage and formed vascular structures. Intravenous administration of AM-expressing EPCs significantly decreased pulmonary vascular resistance compared with EPCs alone (−39%). Kaplan-Meier survival curves demonstrated that rats with pulmonary hypertension transplanted with AM-expressing EPCs had a significantly higher survival rate than those given culture medium or EPCs alone. These findings suggest that AM gene-modified EPCs using gelatin may serve not only as a tissue-engineering tool to reconstruct the pulmonary vasculature, but also as a vehicle for gene delivery to injured pulmonary endothelium. This hybrid cell-gene therapy may be applicable for intractable cardiovascular disease, including ischemic heart disease. Thus genetic manipulation of stem cells opens new avenues for regenerative medicine.

GRANTS

This work was supported by the Research Grant for Cardiovascular Disease (16C-6) from the Ministry of Health, Labor and Welfare, Industrial Technology Research Grant Program in 2003 from New Energy and Industrial Technology Development Organization of Japan, Health and Labor Sciences Research Grants-Genome 005, the Mochida Memorial Foundation for Medical and Pharmaceutical Research, and the Promotion of Fundamental Studies in Health Science of the Organization for Pharmaceutical Safety and Research of Japan.

REFERENCES

1. **Abe M, Sata M, Nishimatsu H, Nagata D, Suzuki E, Terauchi Y, Kadowaki T, Minamino N, Kangawa K, Matsuo H, Hirata Y, and Nagai R.** Adrenomedullin augments collateral development in response to acute ischemia. *Biochem Biophys Res Commun* 306: 10–15, 2003.
2. **Agata J, Zhang JJ, Chao J, and Chao L.** Adrenomedullin gene delivery inhibits neointima formation in rat artery after balloon angioplasty. *Regul Pept* 112: 115–120, 2003.
3. **Archer S and Rich S.** Primary pulmonary hypertension: a vascular biology and translational research "work in progress". *Circulation* 102: 2781–2791, 2000.
4. **Asahara T, Murohara T, Sullivan A, Silver M, van der Zee R, Li T, Witzenbichler B, Schatteman G, and Isner JM.** Isolation of putative progenitor endothelial cells for angiogenesis. *Science* 275: 964–967, 1997.
5. **Belch JJ, Topol EJ, Agnelli G, Bertrand M, Califf RM, Clement DL, Creager MA, Easton JD, Gavin 3rd JR, Greenland P, Hankey G, Hanrath P, Hirsch AT, Meyer J, Smith SC, Sullivan F, Weber MA, Prevention of Atherothrombotic, and Disease Network.** Critical issues in peripheral arterial disease detection and management: a call to action. *Arch Intern Med* 163: 884–892, 2003.
6. **Caron KM and Smithies O.** Extreme hydrops fetalis and cardiovascular abnormalities in mice lacking a functional adrenomedullin gene. *Proc Natl Acad Sci USA* 98: 615–619, 2001.
7. **Chun TH, Itoh H, Ogawa Y, Tamura N, Takaya K, Igaki T, Yamashita J, Doi K, Inoue M, Masatsugu K, Korenaga R, Ando J, and Nakao K.** Shear stress augments expression of C-type natriuretic peptide and adrenomedullin. *Hypertension* 29: 1296–1302, 1997.
8. **Cueille C, Pidoux E, de Vernejoul MC, Ventura-Clapier R, and Garel JM.** Increased myocardial expression of RAMP1 and RAMP3 in rats with chronic heart failure. *Biochem Biophys Res Commun* 294: 340–346, 2002.
9. **Dobrzynski E, Wang C, Chao J, and Chao L.** Adrenomedullin gene delivery attenuates hypertension, cardiac remodeling, and renal injury in deoxycorticosterone acetate-salt hypertensive rats. *Hypertension* 36: 995–1001, 2000.
10. **Feldman LJ, Steg PG, Zheng LP, Chen D, Kearney M, McGarr SE, Barry JJ, Dedieu JF, Perricaudet M, and Isner JM.** Low-efficiency of percutaneous adenovirus-mediated arterial gene transfer in the atherosclerotic rabbit. *J Clin Invest* 95: 2662–2671, 1995.
11. **Fernandez-Sauze S, Delfino C, Mabrouk K, Dussert C, Chinot O, Martin PM, Grisoli F, Ouafik L, and Boudouresque F.** Effects of adrenomedullin on endothelial cells in the multistep process of angiogenesis: involvement of CRLR/RAMP2 and CRLR/RAMP3 receptors. *Int J Cancer* 108: 797–804, 2004.
12. **Fujita Y, Mimata H, Nasu N, Nomura T, Nomura Y, and Nakagawa M.** Involvement of adrenomedullin induced by hypoxia in angiogenesis in human renal cell carcinoma. *Int J Urol* 9: 285–295, 2002.
13. **Fukunaka Y, Iwanaga K, Morimoto K, Kakemi M, and Tabata Y.** Controlled release of plasmid DNA from cationized gelatin hydrogels based on hydrogel degradation. *J Control Release* 80: 333–343, 2002.
14. **Garayoa M, Martinez A, Lee S, Pio R, An WG, Neckers L, Trepel J, Montuenga LM, Ryan H, Johnson R, Gassmann M, and Cuttitta F.** Hypoxia-inducible factor-1 (HIF-1) up-regulates adrenomedullin expression in human tumor cell lines during oxygen deprivation: a possible promotion mechanism of carcinogenesis. *Mol Endocrinol* 14: 848–862, 2000.
15. **Gill M, Dias S, Hattori K, Rivera ML, Hicklin D, Witte L, Girardi L, Yurt R, Himel H, and Rafii S.** Vascular trauma induces rapid but transient mobilization of VEGFR2(+)AC133(+) endothelial precursor cells. *Circ Res* 88: 167–174, 2001.
16. **Hippenstiel S, Witzenrath M, Schmeck B, Hocke A, Krisp M, Krull M, Seybold J, Seeger W, Rascher W, Schutte H, and Suttorp N.** Adrenomedullin reduces endothelial hyperpermeability. *Circ Res* 91: 618–625, 2002.
17. **Hirata Y, Hayakawa H, Suzuki Y, Suzuki E, Ikenouchi H, Kohmoto O, Kimura K, Kitamura K, Eto T, Kangawa K, Matsuo H, and Omata M.** Mechanisms of adrenomedullin-induced vasodilation in the rat kidney. *Hypertension* 25: 790–795, 1995.
18. **Hofbauer KH, Jensen BL, Kurtz A, and Sandner P.** Tissue hypoxygenation activates the adrenomedullin system in vivo. *Am J Physiol Regul Integr Comp Physiol* 278: R513–R519, 2000.
19. **Ichiki Y, Kitamura K, Kangawa K, Kawamoto M, Matsuo H, and Eto T.** Distribution and characterization of immunoreactive adrenomedullin in human tissue and plasma. *FEBS Lett* 338: 6–10, 1994.
20. **Iimuro S, Shindo T, Moriyama N, Amaki T, Niu P, Takeda N, Iwata H, Zhang Y, Ebihara A, and Nagai R.** Angiogenic effects of adrenomedullin in ischemia and tumor growth. *Circ Res* 95: 415–423, 2004.
21. **Imai Y, Shiindo T, Maemura K, Kurihara Y, Nagai R, and Kurihara H.** Evidence for the physiological and pathological roles of adrenomedullin from genetic engineering in mice. *Ann NY Acad Sci* 947: 26–33, 2001.
22. **Ishimitsu T, Nishikimi T, Saito Y, Kitamura K, Eto T, Kangawa K, Matsuo H, Omae T, and Matsuoka H.** Plasma levels of adrenomedullin, a newly identified hypotensive peptide, in patients with hypertension and renal failure. *J Clin Invest* 94: 2158–2161, 1994.
23. **Ishizaka Y, Ishizaka Y, Tanaka M, Kitamura K, Kangawa K, Minamino N, Matsuo H, and Eto T.** Adrenomedullin stimulates cyclic AMP formation in rat vascular smooth muscle cells. *Biochem Biophys Res Commun* 200: 642–646, 1994.

24. Isner JM, Pieczek A, Schainfeld R, Blair R, Haley L, Asahara T, Rosenfield K, Razvi S, Walsh K, and Symes JF. Clinical evidence of angiogenesis after arterial gene transfer of phVEGF165 in patient with ischemic limb. *Lancet* 348: 370–374, 1996.
25. Iwase T, Nagaya N, Fujii T, Itoh T, Ishibashi-Ueda H, Yamagishi M, Miyatake K, Matsumoto T, Kitamura S, and Kangawa K. Adrenomedullin enhances angiogenic potency of bone marrow transplantation in a rat model of hindlimb ischemia. *Circulation* 111: 356–362, 2005.
26. Jain RK. Molecular regulation of vessel maturation. *Nat Med* 9: 685–693, 2003.
27. Jiang BH, Zheng JZ, Aoki M, and Vogt PK. Phosphatidylinositol 3-kinase signaling mediates angiogenesis and expression of vascular endothelial growth factor in endothelial cells. *Proc Natl Acad Sci USA* 97: 1749–1753, 2000.
28. Jougasaki M, Wei CM, McKinley LJ, and Burnett JC Jr. Elevation of circulating and ventricular adrenomedullin in human congestive heart failure. *Circulation* 92: 286–289, 1995.
29. Kakishita M, Nishikimi T, Okano Y, Satoh T, Kyotani S, Nagaya N, Fukushima K, Nakanishi N, Takishita S, Miyata A, Kangawa K, Matsuo H, and Kunieda T. Increased plasma levels of adrenomedullin in patients with pulmonary hypertension. *Clin Sci (Lond)* 96: 33–39, 1999.
30. Kasahara H, Tanaka E, Fukuyama N, Sato E, Sakamoto H, Tabata Y, Ando K, Iseki H, Shinozaki Y, Kimura K, Kuwabara E, Koide S, Nakazawa H, and Mori H. Biodegradable gelatin hydrogel potentiates the angiogenic effect of fibroblast growth factor 4 plasmid in rabbit hindlimb ischemia. *J Am Coll Cardiol* 41: 1056–1062, 2003.
31. Kato H, Shichiri M, Marumo F, and Hirata Y. Adrenomedullin as an autocrine/paracrine apoptosis survival factor for rat endothelial cells. *Endocrinology* 138: 2615–2620, 1997.
32. Kato K, Yin H, Agata J, Yoshida H, Chao L, and Chao J. Adrenomedullin gene delivery attenuates myocardial infarction and apoptosis after ischemia and reperfusion. *Am J Physiol Heart Circ Physiol* 285: H1506–H1514, 2003.
33. Kawai J, Ando K, Tojo A, Shimosawa T, Takahashi K, Onozato ML, Yamasaki M, Ogita T, Nakaoka T, and Fujita T. Endogenous adrenomedullin protects against vascular response to injury in mice. *Circulation* 109: 1147–1153 2004.
34. Kawamoto A, Gwon HC, Iwaguro H, Yamaguchi JI, Uchida S, Masuda H, Silver M, Ma H, Kearney M, Isner JM, and Asahara T. Therapeutic potential of ex vivo expanded endothelial progenitor cells for myocardial ischemia. *Circulation* 103: 634–637, 2001.
35. Kim W, Moon SO, Sung MJ, Kim SH, Lee S, So JN, and Park SK. Angiogenic role of adrenomedullin through activation of Akt, mitogen-activated protein kinase, and focal adhesion kinase in endothelial cells. *FASEB J* 13: 1937–1939, 2003.
36. Kitamura K, Kangawa K, Kawamoto M, Ichiki Y, Nakamura S, Matsuo H, and Eto T. Adrenomedullin: a novel hypotensive peptide isolated from human pheochromocytoma. *Biochem Biophys Res Commun* 192: 553–560, 1993.
37. Marx M, Perlmutter RA, and Madri JA. Modulation of platelet-derived growth factor receptor expression in microvascular endothelial cells during in vitro angiogenesis. *J Clin Invest* 93: 131–139, 1994.
38. McLatchie LM, Fraser NJ, Main MJ, Wise A, Brown J, Thompson N, Solari R, Lee MG, and Foord SM. RAMPs regulate the transport and ligand specificity of the calcitonin-receptor-like receptor. *Nature* 393: 333–339, 1998.
39. Miller MJ, Martinez A, Unsworth EJ, Thiele CJ, Moody TW, Elsasser T, and Cuttitta F. Adrenomedullin expression in human tumor cell lines. Its potential role as an autocrine growth factor. *J Biol Chem* 271: 23345–23351, 1996.
40. Miyao Y, Nishikimi T, Goto Y, Miyazaki S, Daikoku S, Morii I, Matsumoto T, Takishita S, Miyata A, Matsuo H, Kangawa K, and Nonogi H. Increased plasma adrenomedullin levels in patients with acute myocardial infarction in proportion to the clinical severity. *Heart* 79: 39–44, 1998.
41. Miyashita K, Itoh H, Sawada N, Fukunaga Y, Sone M, Yamahara K, Yurugi-Kobayashi T, Park K, and Nakao K. Adrenomedullin provokes endothelial Akt activation and promotes vascular regeneration both in vitro and in vivo. *FEBS Lett* 544: 86–92, 2003.
42. Murohara T, Ikeda H, Duan J, Shintani S, Sasaki K, Eguchi H, Onitsuka I, Matsui K, and Imaizumi T. Transplanted cord blood-derived endothelial precursor cells augment postnatal neovascularization. *J Clin Invest* 105: 1527–1536, 2000.
43. Nagae T, Mukoyama M, Sugawara A, Mori K, Yahata K, Kasahara M, Suganami T, Makino H, Fujinaga Y, Yoshioka T, Tanaka I, and Nakao K. Rat receptor-activity-modifying proteins (RAMPs) for adrenomedullin/CGRP receptor: cloning and upregulation in obstructive nephropathy. *Biochem Biophys Res Commun* 270: 89–93, 2000.
44. Nagaya N, Kangawa K, Kanda M, Uematsu M, Horio T, Fukuyama N, Hino J, Harada-Shiba M, Okumura H, Tabata Y, Mochizuki N, Chiba Y, Nishioka K, Miyatake K, Asahara T, Hara H, and Mori H. Hybrid cell-gene therapy for pulmonary hypertension based on phagocytosing action of endothelial progenitor cells. *Circulation* 108: 889–895, 2003.
45. Nagaya N, Kyotani S, Uematsu M, Ueno K, Oya H, Nakanishi N, Shirai M, Mori H, Miyatake K, and Kangawa K. Effects of adrenomedullin inhalation on hemodynamics and exercise capacity in patients with idiopathic pulmonary arterial hypertension. *Circulation* 109: 351–356, 2004.
46. Nagaya N, Miyatake K, Kyotani S, Nishikimi T, Nakanishi N, and Kangawa K. Pulmonary vasodilator response to adrenomedullin in patients with pulmonary hypertension. *Hypertens Res* 26 Suppl: S141–S146, 2003.
47. Nagaya N, Nishikimi T, Horio T, Yoshihara F, Kanazawa A, Matsuo H, and Kangawa K. Cardiovascular and renal effects of adrenomedullin in rats with heart failure. *Am J Physiol Regul Integr Comp Physiol* 276: R213–R218, 1999.
48. Nagaya N, Nishikimi T, Uematsu M, Satoh T, Oya H, Kyotani S, Sakamaki F, Ueno K, Nakanishi N, Miyatake K, and Kangawa K. Hemodynamic and hormonal effects of adrenomedullin in patients with pulmonary hypertension. *Heart* 84: 653–658, 2000.
49. Nagaya N, Nishikimi T, Uematsu M, Yoshitomi Y, Miyao Y, Miyazaki S, Goto Y, Kojima S, Kuramochi M, Matsuo H, Kangawa K, and Nonogi H. Plasma adrenomedullin as an indicator of prognosis after acute myocardial infarction. *Heart* 81: 483–487, 1999.
50. Nagaya N, Nishikimi T, Yoshihara F, Horio T, Morimoto A, and Kangawa K. Cardiac adrenomedullin gene expression and peptide accumulation after acute myocardial infarction in rats. *Am J Physiol Regul Integr Comp Physiol* 278: R1019–R1026, 2000.
51. Nagaya N, Okumura H, Uematsu M, Shimizu W, Ono F, Shirai M, Mori H, Miyatake K, and Kangawa K. Repeated inhalation of adrenomedullin ameliorates pulmonary hypertension and survival in monocrotaline rats. *Am J Physiol Heart Circ Physiol* 285: H2125–H2131, 2003.
52. Nagaya N, Satoh T, Nishikimi T, Uematsu M, Furuichi S, Sakamaki F, Oya H, Kyotani S, Nakanishi N, Goto Y, Masuda Y, Miyatake K, and Kangawa K. Hemodynamic, renal, and hormonal effects of adrenomedullin infusion in patients with congestive heart failure. *Circulation* 101: 498–503, 2000.
53. Nakayama M, Takahashi K, Murakami O, Shirato K, and Shibahara S. Induction of adrenomedullin by hypoxia and cobalt chloride in human colorectal carcinoma cells. *Biochem Biophys Res Commun* 243: 514–517, 1998.
54. Nikitenko LL, Smith DM, Bicknell R, and Rees MC. Transcriptional regulation of the CRLR gene in human microvascular endothelial cells by hypoxia. *FASEB J* 17: 1499–501, 2003.
55. Nishikimi T, Saito Y, Kitamura K, Ishimitsu T, Eto T, Kangawa K, Matsuo H, Omae T, and Matsuoka H. Increased plasma levels of adrenomedullin in patients with heart failure. *J Am Coll Cardiol* 26: 1424–1431, 1995.
56. Nishikimi T, Tadokoro K, Mori Y, Wang X, Akimoto K, Yoshihara F, Minamino N, Kangawa K, and Matsuoka H. Ventricular adrenomedullin system in the transition from LVH to heart failure in rats. *Hypertension* 41: 512–518, 2003.
57. Nishikimi T, Yoshihara F, Horinaka S, Kobayashi N, Mori Y, Tadokoro K, Akimoto K, Minamino N, Kangawa K, and Matsuoka H. Chronic administration of adrenomedullin attenuates transition from left ventricular hypertrophy to heart failure in rats. *Hypertension* 42: 1034–1041, 2003.
58. Nishimatsu H, Suzuki E, Nagata D, Moriyama N, Satonaka H, Walsh K, Sata M, Kangawa K, Matsuo H, Goto A, Kitamura T, and Hirata Y. Adrenomedullin induces endothelium-dependent vasorelaxation via the phosphatidylinositol 3-kinase/Akt-dependent pathway in rat aorta. *Circ Res* 89: 63–70, 2001.
59. Nishio K, Akai Y, Murao Y, Doi N, Ueda S, Tabuse H, Miyamoto S, Dohi K, Minamino N, Shoji H, Kitamura K, Kangawa K, and Matsuo H. Increased plasma concentrations of adrenomedullin correlate with relaxation of vascular tone in patients with septic shock. *Crit Care Med* 25: 953–957, 1997.

60. Oehler MK, Hague S, Rees MC, and Bicknell R. Adrenomedullin promotes formation of xenografted endometrial tumors by stimulation of autocrine growth and angiogenesis. *Oncogene* 21: 2815–2821, 2002.
61. Okumura H, Nagaya N, Itoh T, Okano I, Hino J, Mori K, Tsukamoto Y, Ishibashi-Ueda H, Miwa S, Tambara K, Toyokuni S, Yutani C, and Kangawa K. Adrenomedullin infusion attenuates myocardial ischemia/reperfusion injury through the phosphatidylinositol 3-kinase/Akt-dependent pathway. *Circulation* 109: 242–248, 2004.
62. Rademaker MT, Cameron VA, Charles CJ, Lainchbury JG, Nicholls MG, and Richards AM. Adrenomedullin and heart failure. *Regul Pept* 112: 51–60, 2003.
63. Rademaker MT, Charles CJ, Cooper GJ, Coy DH, Espiner EA, Lewis LK, Nicholls MG, and Richards AM. Combined angiotensin-converting enzyme inhibition and adrenomedullin in an ovine model of heart failure. *Clin Sci (Lond)* 102: 653–660, 2002.
64. Rademaker MT, Charles CJ, Espiner EA, Nicholls MG, and Richards AM. Long-term adrenomedullin administration in experimental heart failure. *Hypertension* 40: 667–672, 2002.
65. Rademaker MT, Charles CJ, Lewis LK, Yandle TG, Cooper GJ, Coy DH, Richards AM, and Nicholls MG. Beneficial hemodynamic and renal effects of adrenomedullin in an ovine model of heart failure. *Circulation* 96: 1983–1990, 1997.
66. Ribatti D, Guidolin D, Conconi MT, Nico B, Baiguera S, Parnigotto PP, Vacca A, and Nussdorfer GG. Vinblastine inhibits the angiogenic response induced by adrenomedullin in vitro and in vivo. *Oncogene* 22: 6458–6461, 2003.
67. Rich S, Dantzker DR, Ayres SM, Bergofsky EH, Brundage BH, Detre KM, Fishman AP, Goldring RM, Groves BM, Koerner SK, Levy PC, Reid LM, Vreim CE, and Williams GW. Primary pulmonary hypertension : a national prospective study. *Ann Intern Med* 107: 216–223, 1987.
68. Schweigerer L, Neufeld G, Friedman J, Abraham JA, Fiddes JC, and Gospodarowicz D. Capillary endothelial cells express basic fibroblast growth factor, a mitogen that promotes their own growth. *Nature* 325: 257–259, 1987.
69. Shimosawa T, Shibagaki Y, Ishibashi K, Kitamura K, Kangawa K, Kato S, Ando K, and Fujita T. Adrenomedullin, an endogenous peptide, counteracts cardiovascular damage. *Circulation* 105:106–111, 2002.
70. Shindo T, Kurihara Y, Nishimatsu H, Moriyama N, Kakoki M, Wang Y, Imai Y, Ebihara A, Kuwaki T, Ju KH, Minamino N, Kangawa K, Ishikawa T, Fukuda M, Akimoto Y, Kawakami H, Imai T, Morita H, Yazaki Y, Nagai R, Hirata Y, and Kurihara H. Vascular abnormalities and elevated blood pressure in mice lacking adrenomedullin gene. *Circulation* 104: 1964–1971, 2001.
71. Shintani S, Murohara T, Ikeda H, Ueno T, Sasaki K, Duan J, and Imaizumi T. Augmentation of postnatal neovascularization with autologous bone marrow transplantation. *Circulation* 103: 897–903, 2001.
72. St George JA. Gene therapy progress and prospects: adenoviral vectors. *Gene Ther* 10: 1135–1141, 2003.
73. Sugo S, Minamino N, Shoji H, Kangawa K, Kitamura K, Eto T, and Matsuo H. Interleukin-1, tumor necrosis factor and lipopolysaccharide additively stimulate production of adrenomedullin in vascular smooth muscle cells. *Biochem Biophys Res Commun* 207: 25–32, 1995.
74. Suri C, Jones PF, Patan S, Bartunkova S, Maisonpierre PC, Davis S, Sato TN, and Yancopoulos GD. Requisite role of angiopoietin-1, a ligand for the TIE2 receptor, during embryonic angiogenesis. *Cell* 87: 1171–1180, 1996.
75. Suzuki Y, Horio T, Hayashi T, Nonogi H, Kitamura K, Eto T, Kangawa K, and Kawano Y. Plasma adrenomedullin concentration is increased in patients with peripheral arterial occlusive disease associated with vascular inflammation. *Regul Pept* 118: 99–104, 2004.
76. Tabata Y and Ikada Y. Macrophage activation through phagocytosis of muramyl dipeptide encapsulated in gelatin microspheres. *J Pharm Pharmacol* 39: 698–704, 1987.
77. Tabata Y, Nagano A, and Ikada Y. Biodegradation of hydrogel carrier incorporating fibroblast growth factor. *Tissue Eng* 5: 127–138, 1999.
78. Tadokoro K, Nishikimi T, Mori Y, Wang X, Akimoto K, and Matsuoka H. Altered gene expression of adrenomedullin and its receptor system and molecular forms of tissue adrenomedullin in left ventricular hypertrophy induced by malignant hypertension. *Regul Pept* 112: 71–78, 2003.
79. Takahashi T, Kalka C, Masuda H, Chen D, Silver M, Kearney M, Magner M, Isner JM, and Asahara T. Ischemia- and cytokine-induced mobilization of bone marrow-derived endothelial progenitor cells for neovascularization. *Nat Med* 5: 434–438, 1999.
80. Takeshita S, Zheng LP, Brogi E, Kearney M, Pu LQ, Bunting S, Ferrara N, Symes JF, and Isner JM. Therapeutic angiogenesis. A single intra-arterial bolus of vascular endothelial growth factor augments revascularization in a rabbit ischemic hind limb model. *J Clin Invest* 93: 662–670, 1994.
81. Tokunaga N, Nagaya N, Shirai M, Tanaka E, Ishibashi-Ueda H, Harada-Shiba M, Kanda M, Ito T, Shimizu W, Tabata Y, Uematsu M, Nishigami K, Sano S, Kangawa K, and Mori H. Adrenomedullin gene transfer induces therapeutic angiogenesis in a rabbit model of chronic hind limb ischemia: benefits of a novel nonviral vector, gelatin. *Circulation* 109: 526–531, 2004.
82. Totsune K, Takahashi K, Mackenzie HS, Murakami O, Arihara Z, Sone M, Mouri T, Brenner BM, and Ito S. Increased gene expression of adrenomedullin and adrenomedullin-receptor complexes, receptor-activity modifying protein (RAMP)2 and calcitonin-receptor-like receptor (CRLR) in the hearts of rats with congestive heart failure. *Clin Sci (Lond)* 99: 541–546, 2000.
83. Wang C, Dobrzynski E, Chao J, and Chao L. Adrenomedullin gene delivery attenuates renal damage and cardiac hypertrophy in Goldblatt hypertensive rats. *Am J Physiol Renal Physiol* 280: F964–F971, 2001.
84. Yamasaki M, Kawai J, Nakaoka T, Ogita T, Tojo A, and Fujita T. Adrenomedullin overexpression to inhibit cuff-induced arterial intimal formation. *Hypertension* 41: 302–307, 2003.
85. Yin H, Chao L, and Chao J. Adrenomedullin protects against myocardial apoptosis after ischemia/reperfusion through activation of Akt-GSK signaling. *Hypertension* 43: 109–116, 2004.
86. Zudaire E, Martinez A, and Cuttitta F. Adrenomedullin and cancer. *Regul Pept* 112: 175–183, 2003.

Superposition of x-ray spectra using a brass-target plasma triode

Haruo Obara*[a], Eiichi Sato[b], Yasuomi Hayasi[b], Etsuro Tanaka[c], Hidezo Mori[d], Toshiaki Kawai[e], Takashi Inoue[f], Akira Ogawa[f], Kazuyoshi Takayama[g] and Hideaki Ido[h]

[a] Department of Radiological Technology, College of Medical Science, Tohoku University, 1-1 Seiryocho, Sendai 980-0872, Japan
[b] Department of Physics, Iwate Medical University, 3-16-1 Honchodori, Morioka 020-0015, Japan
[c] Department of Nutritional Science, Faculty of Applied Bio-science, Tokyo University of Agriculture, 1-1-1 Sakuragaoka, Setagaya-ku 156-8502, Japan
[d] Department of Cardiac Physiology, National Cardiovascular Center Research Institute, 5-7-1 Fujishirodai, Suita, Osaka 565-8565 Japan
[e] Electron Tube Division #2, Hamamatsu Photonics K. K., 314-5 Shimokanzo, Iwata 438-0193, Japan
[f] Department of Neurosurgery, School of Medicine, Iwate Medical University, 19-1 Uchimaru, Morioka 020-8505, Japan
[g] Shock Wave Research Center, Institute of Fluid Science, Tohoku University, 2-1-1 Katahira, Sendai 980-8577, Japan
[h] Department of Applied Physics and Informatics, Faculty of Engineering, Tohoku Gakuin University, 1-13-1 Chuo, Tagajo 985-8537, Japan

ABSTRACT

In the plasma flash x-ray generator, a 200 nF condenser is charged up to 50 kV by a power supply, and flash x-rays are produced by the discharging. The x-ray tube is a demountable triode with a brass target containing 65% copper and 35% zinc by weight, and the turbomolecular pump evacuates air from the tube with a pressure of approximately 1 mPa. Target evaporation leads to the formation of weakly ionized linear plasma, consisting of metal ions and electrons, around the fine target, and intense characteristic x-rays are produced. At a charging voltage of 50 kV, the maximum tube voltage was almost equal to the charging voltage of the main condenser, and the peak current was about 15 kA. When the charging voltage was increased, the linear plasma formed, and the K-series characteristic x-ray intensities of zinc Kα, copper Kα, and copper Kβ lines increased substantially. However hardly any zinc Kβ lines were detected. The x-ray pulse widths were approximately 700 ns, and the time-integrated x-ray intensity was approximately 1.2 mGy at 1.0 m from the x-ray source with a charging voltage of 50 kV.

Keywords: flash x-ray, plasma x-ray, weakly ionized linear plasma, characteristic x-rays, x-ray superposition

1. INTRODUCTION

Conventional flash x-ray generators[1] utilize high-voltage condensers and cold-cathode x-ray tubes and produce extremely short x-ray pulses with durations of less than 1 μs. Because the high-voltage durability substantially increases under the pulsed operation, the maximum photon energy of flash x-rays has been increased to 1 MeV or beyond so as to perform military applications utilizing surge Marx generators in conjunction with diodes.
In order to perform biomedical radiography, we have developed several different flash x-ray generators[2-5] corresponding to specific radiographic objectives, and we have succeeded in producing clean K-series characteristic x-rays of nickel and copper from weakly ionized linear plasma using a plasma triode.[6-9] Subsequently, because we have confirmed the irradiations of clean K-series characteristic x-rays of molybdenum using a compact flash x-ray generator with a disk-cathode diode,[10,11] an intense plasma diode have been developed to produce high-photon-energy characteristic x-rays of molybdenum, cerium,[12] tantalum, and tungsten. In particular, the tantalum K rays[13] have been applied to high-speed K-edge angiography using gadolinium-based contrast media.

Ultrafast X-Ray Detectors, High-Speed Imaging, and Applications, edited by Stuart Kleinfelder, Dennis L. Paisley, Zenghu Chang, Jean-Claude Kieffer, Jerome B. Hastings, Proc. of SPIE Vol. 5920 (SPIE, Bellingham, WA, 2005) · 0277-786X/05/$15 · doi: 10.1117/12.620207

On the other hand, we are very interested in the superposition of characteristic x-rays[14] using weakly ionized plasma in order to perform wide-photon-energy or energy subtraction radiography. In particular, the absorption of K rays in the plasma consisting of electrons and two-element metal ions should be investigated. Furthermore, because we have confirmed the irradiation of higher harmonic hard x-rays using nickel and copper targets, the x-ray spectra with photon energies beyond the K edges should be measured.
In this paper, we describe a plasma flash x-ray generator utilizing a brass-target radiation tube, used to perform a preliminary experiment for the superposition of K-series characteristic x-rays in weakly ionized plasma and for producing their higher harmonic hard x-rays.

2. GENERATOR

2.1 High-voltage circuit

Figure 1 shows a block diagram of a high-intensity plasma flash x-ray generator. The generator consists of the following essential components: a high-voltage power supply, a high-voltage condenser with a capacity of approximately 200 nF, a turbomolecular pump, a krytron pulse generator as a trigger device, and a flash x-ray tube. In this generator, a low-impedance transmission line is employed in order to increase maximum tube current (Fig. 2). The high-voltage main condenser is charged up to 50 kV by the power supply, and electric charges in the condenser are discharged to the tube after triggering the cathode electrode with the trigger device. The plasma flash x-rays are then produced.

2.2 X-ray tube

The x-ray tube is a demountable cold-cathode triode that is connected to the turbomolecular pump with a pressure of approximately 1 mPa (Fig. 3). This tube consists of the following major parts: a pipe-shaped graphite cathode with a bore diameter of 10.0 mm, a trigger electrode made from copper wire, a brass focusing electrode, a stainless-steel vacuum chamber, a nylon insulator, a polyethylene terephthalate (Mylar) x-ray window 0.25 mm in thickness, and a 4.0-mm-diameter rod brass target containing 65% copper and 35% zinc by weight. The distance between the target and cathode electrodes is approximately 20 mm, and the trigger electrode is set in the cathode electrode. As electron beams from the cathode electrode are roughly converged to the target by the focusing electrode, evaporation leads to the formation of weakly ionized linear plasma, consisting of metal ions and electrons, around the fine target.

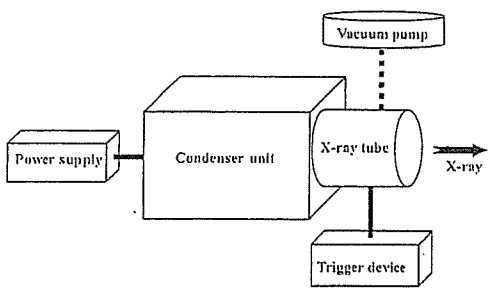

Figure 1: Block diagram of the high-intensity plasma flash x-ray generator.

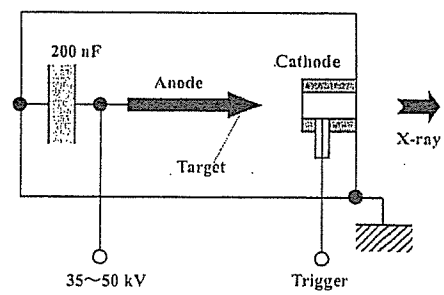

Figure 2: Circuit diagram of the flash x-ray generator.

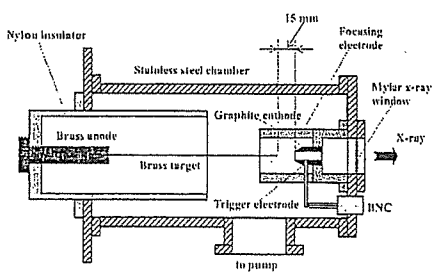

Figure 3: Schematic drawing of the flash x-ray tube with a brass target.

3. CHARACTERISTICS

3.1 Tube voltage and current

Tube voltage and current were measured by a high-voltage divider with an input impedance of 1 GΩ and a current transformer, respectively. Figure 4 shows the time relation between the tube voltage and current. At the indicated charging voltages, they roughly displayed damped oscillations. When the charging voltage was increased, both the maximum tube voltage and current increased. At a charging voltage of 50 kV, the maximum tube voltage was almost equal to the charging voltage of the main condenser, and the maximum tube current was approximately 15 kA.

3.2 X-ray output

X-ray output pulse was detected using a combination of a plastic scintillator and a photomultiplier (Fig. 5). The x-ray pulse height substantially increased with corresponding increases in the charging voltage. The x-ray pulse widths were about 700 ns, and the time-integrated x-ray intensity measured by a thermoluminescence dosimeter (Kyokko TLD Reader 1500 with MSO-S elements without energy compensation) had a value of approximately 1.2 mGy at 1.0 m from the x-ray source with a charging voltage of 50 kV.

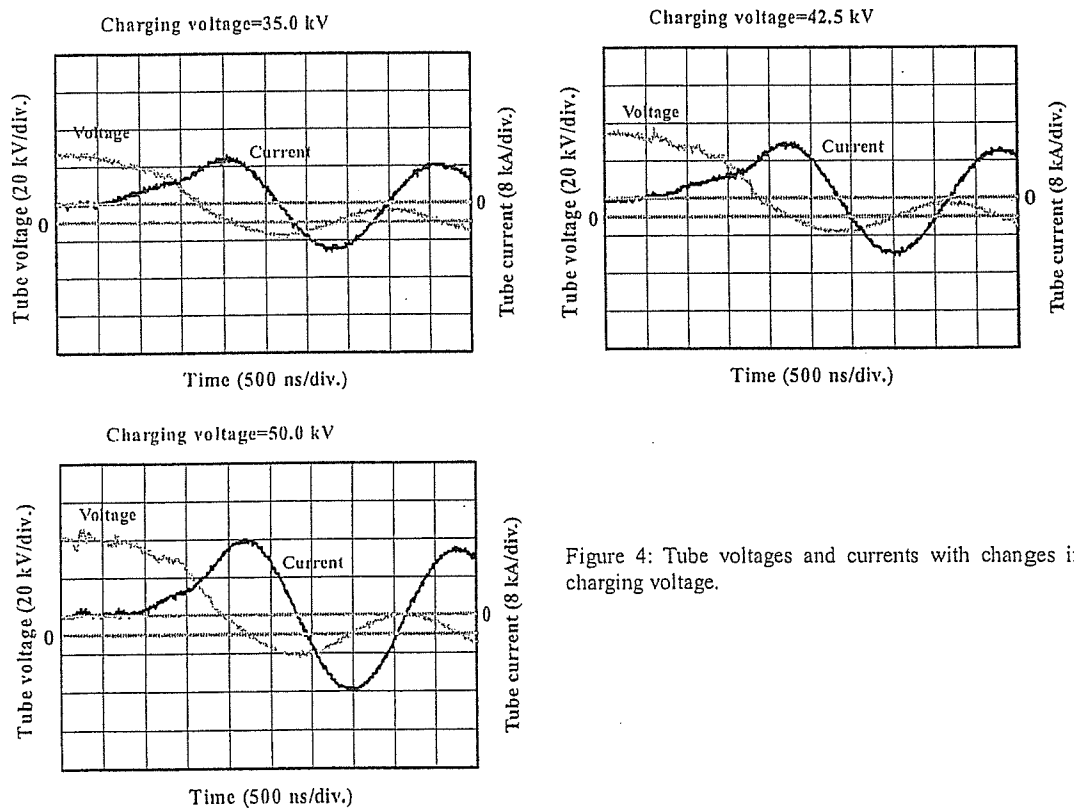

Figure 4: Tube voltages and currents with changes in the charging voltage.

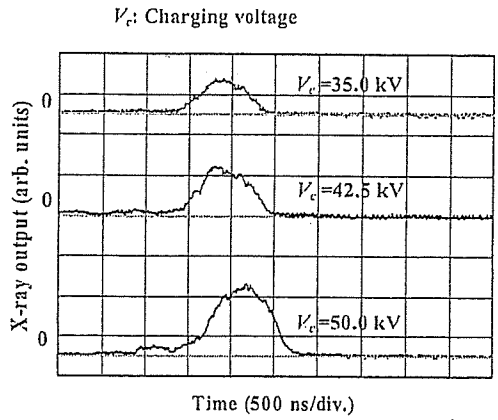

Figure 5: X-ray outputs at the indicated conditions.

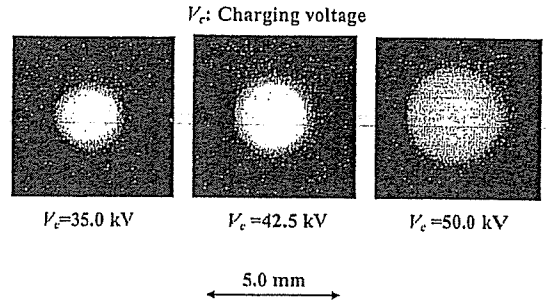

Figure 6: Images of plasma x-ray source.

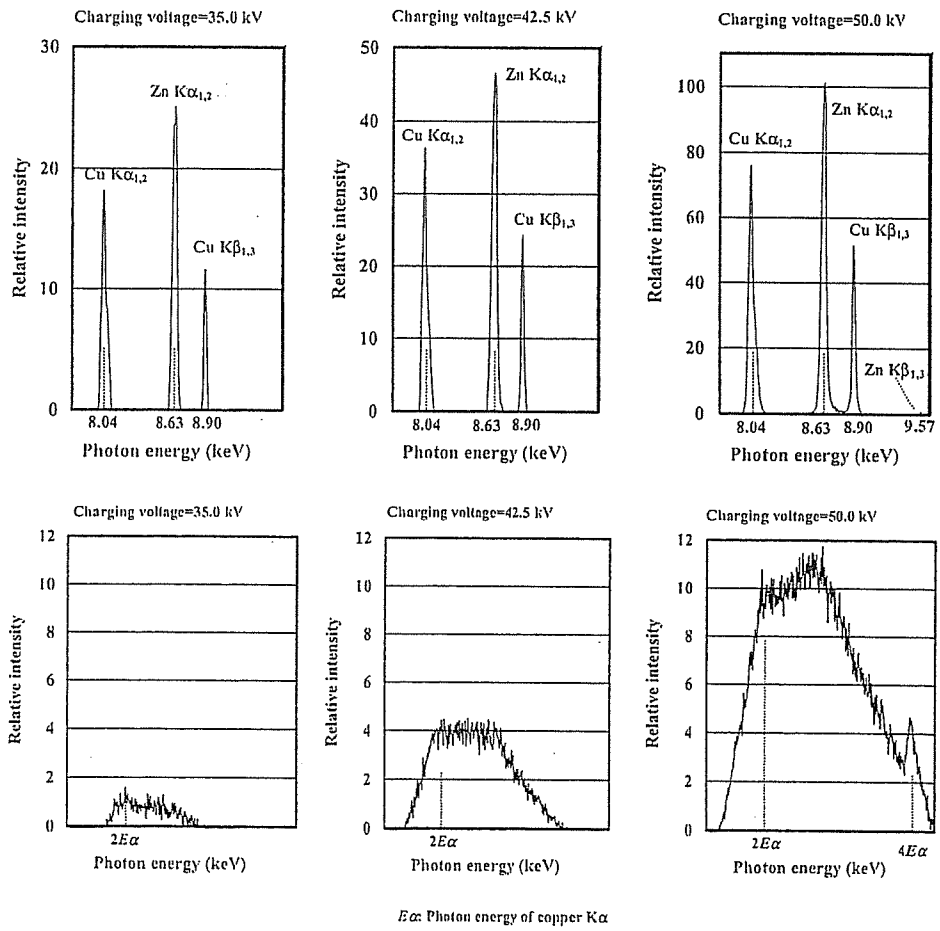

Figure 7: X-ray spectra at the indicated conditions.

3.3 X-ray source

In order to roughly observe images of the plasma x-ray source in the detector plane, we employed a 100-μm-diameter pinhole camera and an x-ray film (Polaroid XR-7) (Fig. 6). When the charging voltage was increased, the plasma x-ray source grew, and both spot dimension and intensity increased. Because the x-ray intensity is the highest at the center of the target, both the dimension and intensity decreased according to both increases in the thickness of a filter for absorbing x-rays and decreases in the pinhole diameter.

3.4 X-ray spectra

X-ray spectra from the plasma source were measured by a transmission-type spectrometer with a lithium fluoride curved crystal 0.5 mm in thickness. The spectra were taken by a computed radiography (CR) system[15] with a wide dynamic range, and relative x-ray intensity was calculated from Dicom digital data.

Figure 7 shows measured spectra from weakly ionized metal plasma. We observed sharp lines of K-series characteristic x- rays of copper Kα, copper Kβ and zinc Kα lines. However, zinc Kβ and bremsstrahlung rays were hardly detected. The characteristic x-ray intensity substantially increased with corresponding increases in the charging voltage. In the high-photon-energy region, higher harmonic hard x-rays with photon energies of approximately $2E_\alpha$ and $4E_\alpha$ were observed. Here, E_α is the average photon energies of copper Kα lines.

4. RADIOGRAPHY

The plasma radiography was performed by the CR system (Konica Regius 150) without using a filter, and the charging voltage and the distance (between the x-ray source and imaging plate) were 501 kV and 1.2 m, respectively.

Figure 8 shows radiograms of tungsten wires coiled around a pipe made of polymethyl methacrylate. Although the image contrast increased with increases in the wire diameter, a 50-μm-diameter wire could be observed. Next, the image of aluminum grains falling into a polypropylene beaker from a glass test tube is shown in Fig. 9. Because the x-ray duration was approximately 700 ns, the stop-motion image of grains could be obtained.

Figures 10 and 11 show angiograms of a rabbit heart and a thigh, respectively. In angiography, iodine-based microspheres of 15 μm in diameter were used, and fine blood vessels of about 100 μm are clearly visible.

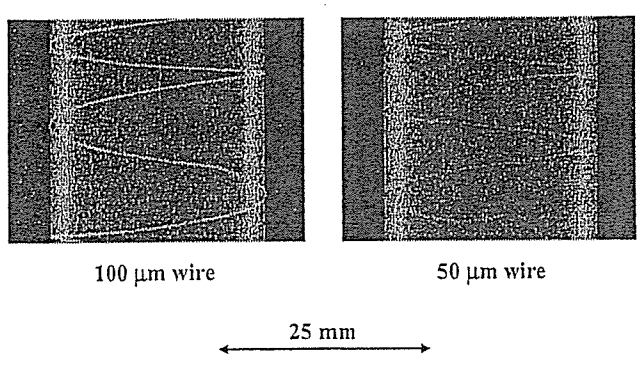

Figure 8: Radiograms of tungsten wires coiled around pipes made of polymethyl methacrylate.

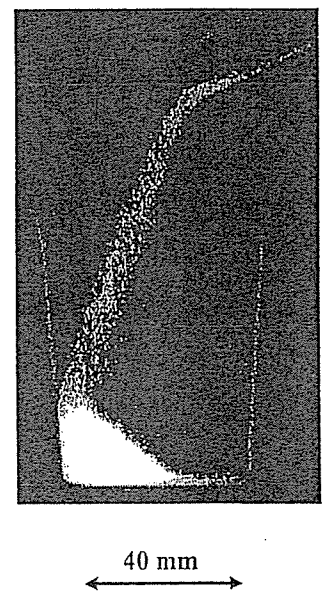

Figure 9: Radiogram of aluminum grains from a glass test tube.

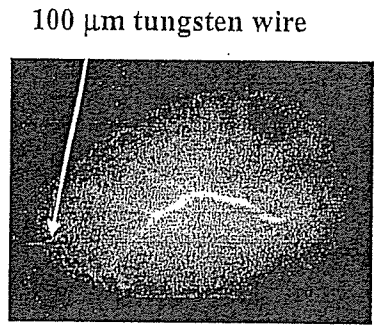

Figure 10: Angiogram of a rabbit heart.

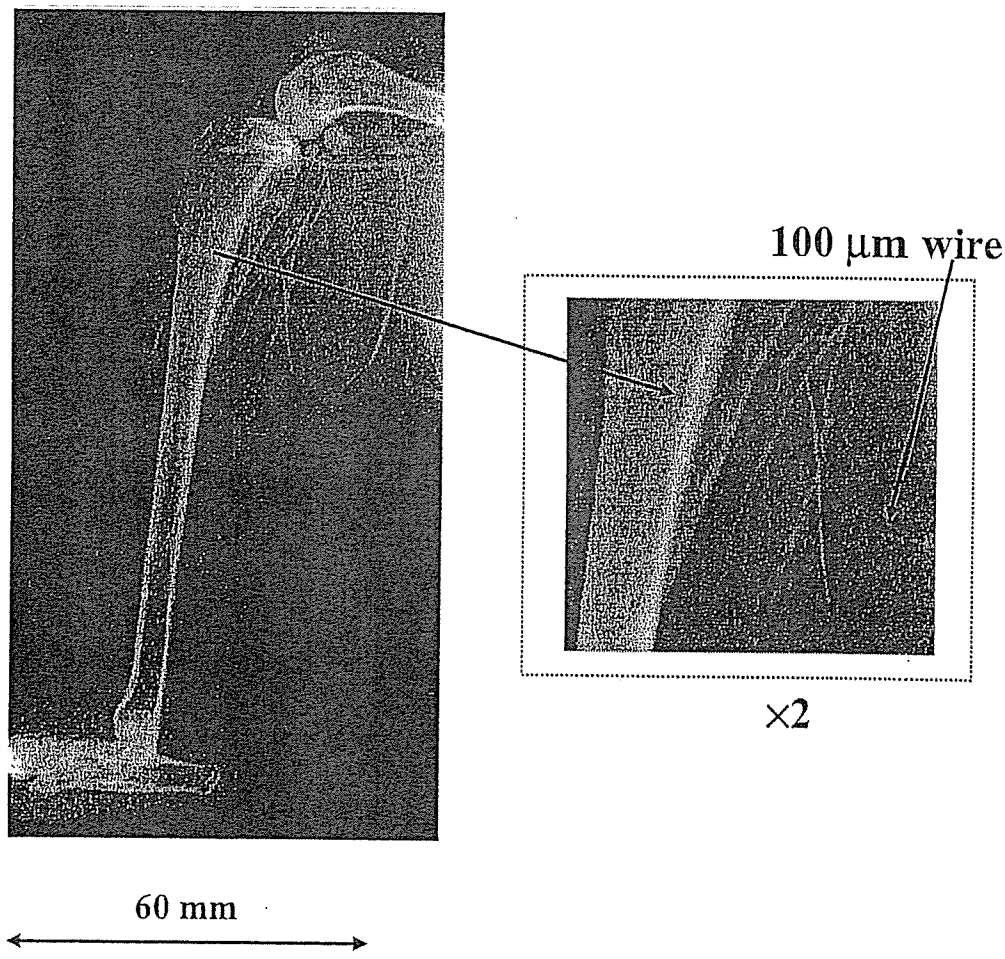

Figure 11: Angiogram of a rabbit thigh.

5. CONCLUSIONS AND OUTLOOK

Regarding the spectrum measurement, although we confirmed clean copper Kα, copper Kβ and zinc Kα lines, zinc Kβ lines were hardly observed. Because weakly ionized zinc plasma (ion) transmits zinc Kβ lines easily, the lines were absorbed by copper plasma. In high-photon-energy region, although we could not observe clean higher harmonics, bremsstrahlung x-rays with photon energies approximately $2E_\alpha$ and $4E_\alpha$ were left in cases where a high charging voltage of approximately 50 kV was applied.

From the experimental results, because the x-ray spectra with photon energies just beyond copper K edge are absorbed effectively by the copper plasma, zinc Kβ rays are useful to produce copper fluorescent rays. In addition, we are very interested in the results using a capillary-type target for forming weakly ionized linear plasma.

In this research, we obtained sufficient characteristic x-ray intensity per pulse for CR radiography, and the generator produced number of characteristic photons was approximately 1×10^8 photons/cm^2 at 1.0 m per pulse. In addition, since the photon energy of characteristic x-rays can be controlled by changing target elements, various quasi-monochromatic high-speed radiographies, such as flash energy subtraction radiography using a metal filter and wide-photon-energy radiography, will be possible.

ACKNOWLEDGMENT

This work was supported by Grants-in-Aid for Scientific Research (13470154, 13877114, 16591181, and 16591222) and Advanced Medical Scientific Research from MECSST, Health and Labor Sciences Research Grants (RAMT-nano-001, RHGTEFB-genome-005 and RHGTEFB-saisei-003), Grants from the Keiryo Research Foundation, The Promotion and Mutual Aid Corporation for Private Schools of Japan, Japan Science and Technology Agency (JST), and the New Energy and Industrial Technology Development Organization (NEDO, Industrial Technology Research Grant Program in '03).

REFERENCES

1. R. Germer, "X-ray flash techniques," *J. Phys. E: Sci. Instrum.*, **12**, 336-350, 1979.
2. E. Sato, S. Kimura, S. Kawasaki, H. Isobe, K. Takahashi, Y. Tamakawa and T. Yanagisawa, "Repetitive flash x-ray generator utilizing a simple diode with a new type of energy-selective function," *Rev. Sci. Instrum.*, **61**, 2343-2348, 1990.
3. A. Shikoda, E. Sato, M. Sagae, T. Oizumi, Y. Tamakawa and T. Yanagisawa, "Repetitive flash x-ray generator having a high-durability diode driven by a two-cable-type line pulser," *Rev. Sci. Instrum.*, **65**, 850-856, 1994.
4. E. Sato, K. Takahashi, M. Sagae, S. Kimura, T. Oizumi, Y. Hayasi, Y. Tamakawa and T. Yanagisawa, "Sub-kilohertz flash x-ray generator utilizing a glass-enclosed cold-cathode triode," *Med. & Biol. Eng. & Comput.*, **32**, 289-294, 1994.
5. K. Takahashi, E. Sato, M. Sagae, T. Oizumi, Y. Tamakawa and T. Yanagisawa, "Fundamental study on a long-duration flash x-ray generator with a surface-discharge triode," *Jpn. J. Appl. Phys.*, **33**, 4146-4151, 1994.
6. E. Sato, Y. Hayasi, R. Germer, E. Tanaka, H. Mori, T. Kawai, H. Obara, T. Ichimaru, K. Takayama and H. Ido, "Irradiation of intense characteristic x-rays from weakly ionized linear molybdenum plasma," *Jpn. J. Med. Phys.*, **23**, 123-131, 2003.
7. E. Sato, Y. Hayasi, R. Germer, E. Tanaka, H. Mori, T. Kawai, T. Ichimaru, K. Takayama and H. Ido, "Quasi-monochromatic flash x-ray generator utilizing weakly ionized linear copper plasma," *Rev. Sci. Instrum.*, **74**, 5236-5240, 2003.
8. E. Sato, Y. Hayasi, R. Germer, E. Tanaka, H. Mori, T. Kawai, T. Ichimaru, S. Sato, K. Takayama and H. Ido, "Sharp characteristic x-ray irradiation from weakly ionized linear plasma," *J. Electron Spectrosc. Related Phenom.*, **137-140**, 713-720, 2004.
9. E. Sato, E. Tanaka, H. Mori, T. Kawai,S. Sato and K. Takayama, "Clean monochromatic x-ray irradiation from weakly ionized linear copper plasma," *Opt. Eng.*, 44, 049002-1-6, 2005.
10. E. Sato, M. Sagae, E. Tanaka, Y. Hayasi, R. Germer, H. Mori, T. Kawai, T. Ichimaru, S. Sato, K. Takayama and H. Ido: Quasi-monochromatic flash x-ray generator utilizing a disk-cathode molybdenum tube, *Jpn. J. Appl. Phys.*, 43, 7324-7328, 2004.
11. E. Sato, E. Tanaka, H. Mori, T. Kawai, T. Ichimaru, S. Sato, K. Takayama and H. Ido, "Compact monochromatic flash x-ray generator utilizing a disk-cathode molybdenum tube," *Med. Phys.*, **32**, 49-54, 2005.
12. E. Sato, R. Germer, E. Tanaka, H. Mori, T. Kawai, T. Ichimaru, S. Sato, H. Ojima, K. Takayama and H. Ido,